Dissociation and Regeneration of Charmonia within microscopic Langevin simulations

Exotic Quarkonia in Heavy-ion Collisions
MITP, February 04, 2026

Naomi Oei

In collaboration with Juan Torres-Rincon, Hendrik van Hees and Carsten Greiner

Based on PhysRevD.111.074012

Motivation

Heavy Quarkonium as a QGP Probe

- HQ- bound states probe **in-medium QCD forces** and **transport of heavy quarks**
- Key competition in AA: **suppression vs. regeneration**

  ➡ controlled by $c\bar{c}/b\bar{b}$ - abundance

- Flow observables: constrain HQ-coupling to the medium

➡**This work:** focus on dynamical regeneration in a Langevin transport framework

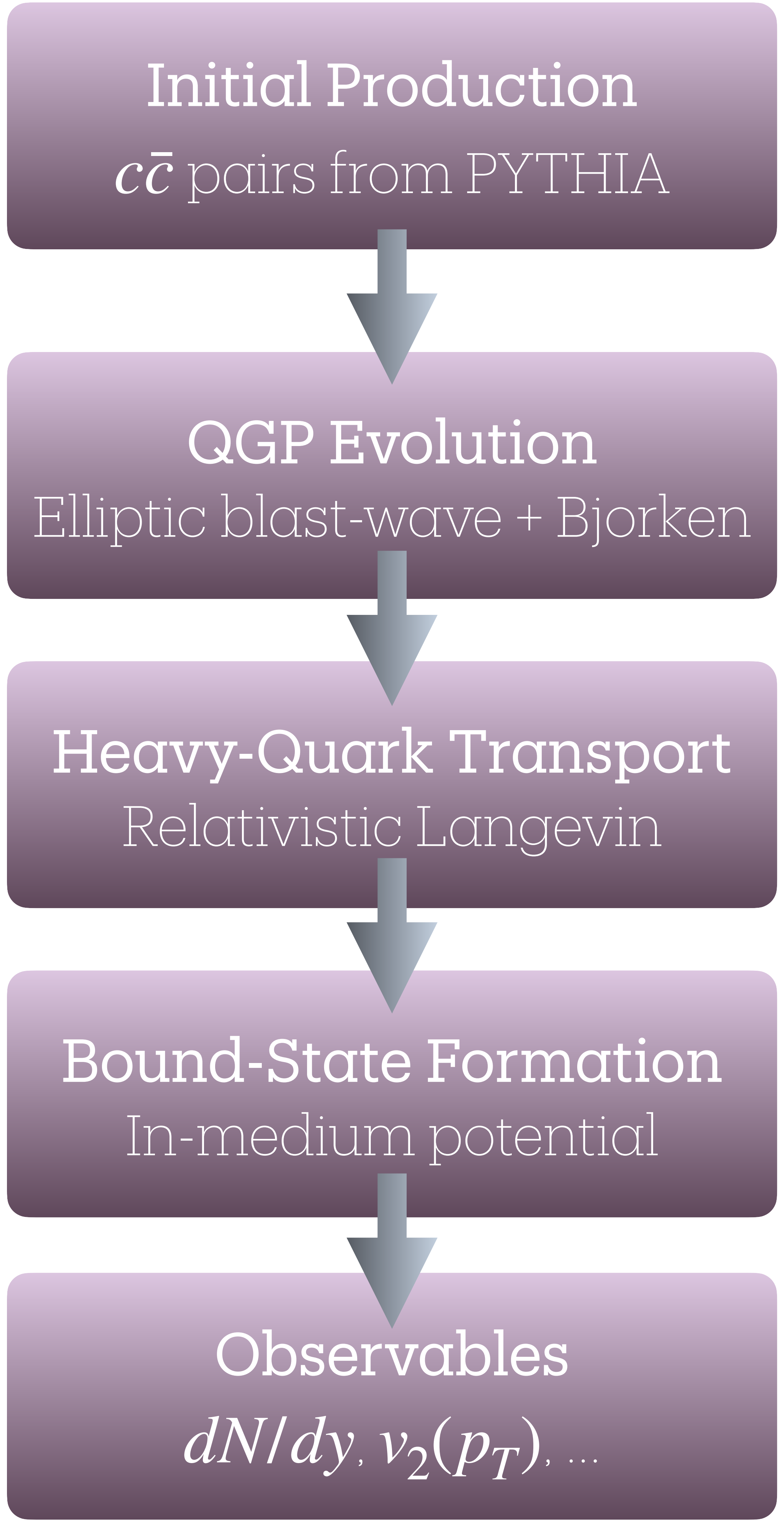

Motivation

Suppression and Regeneration

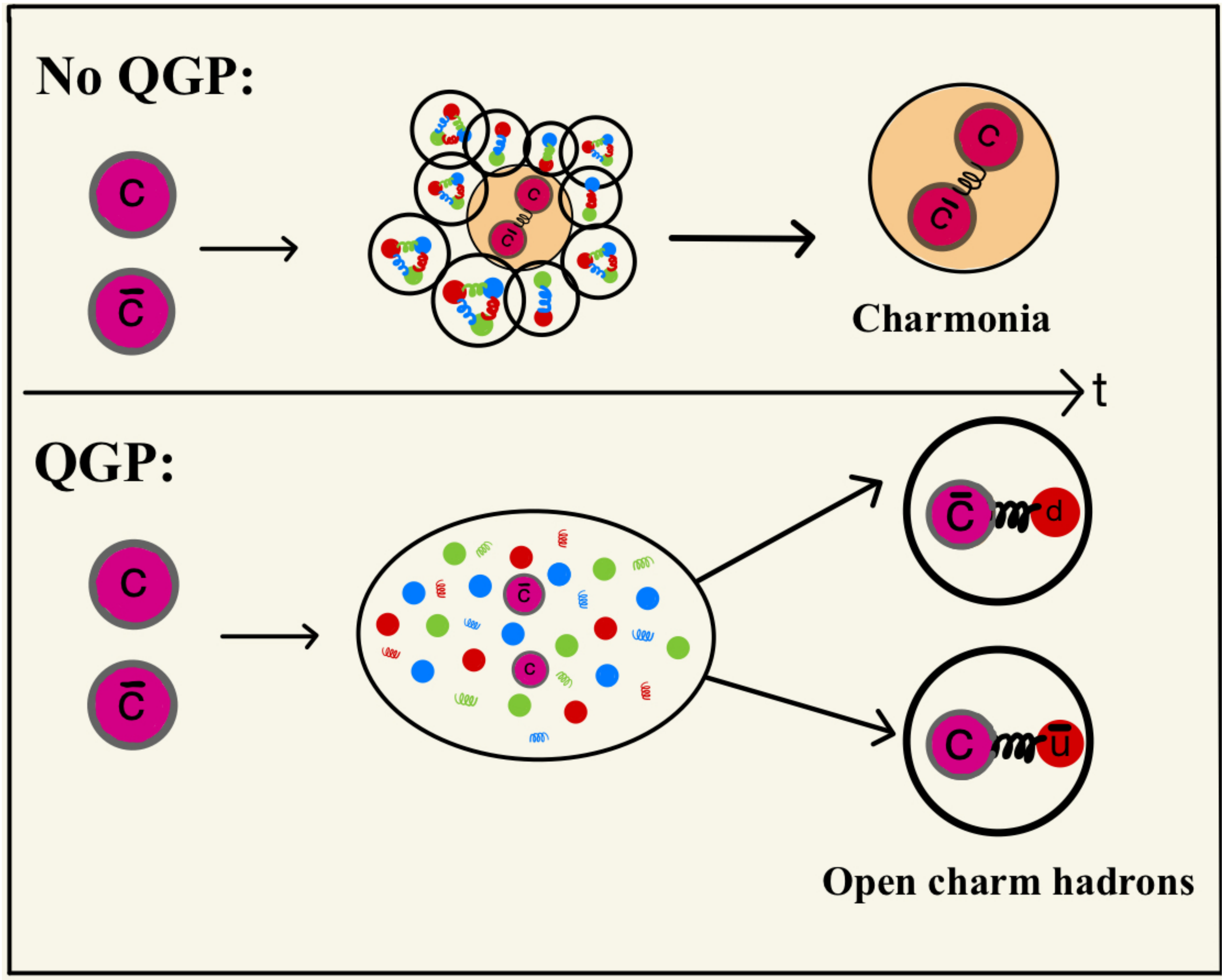

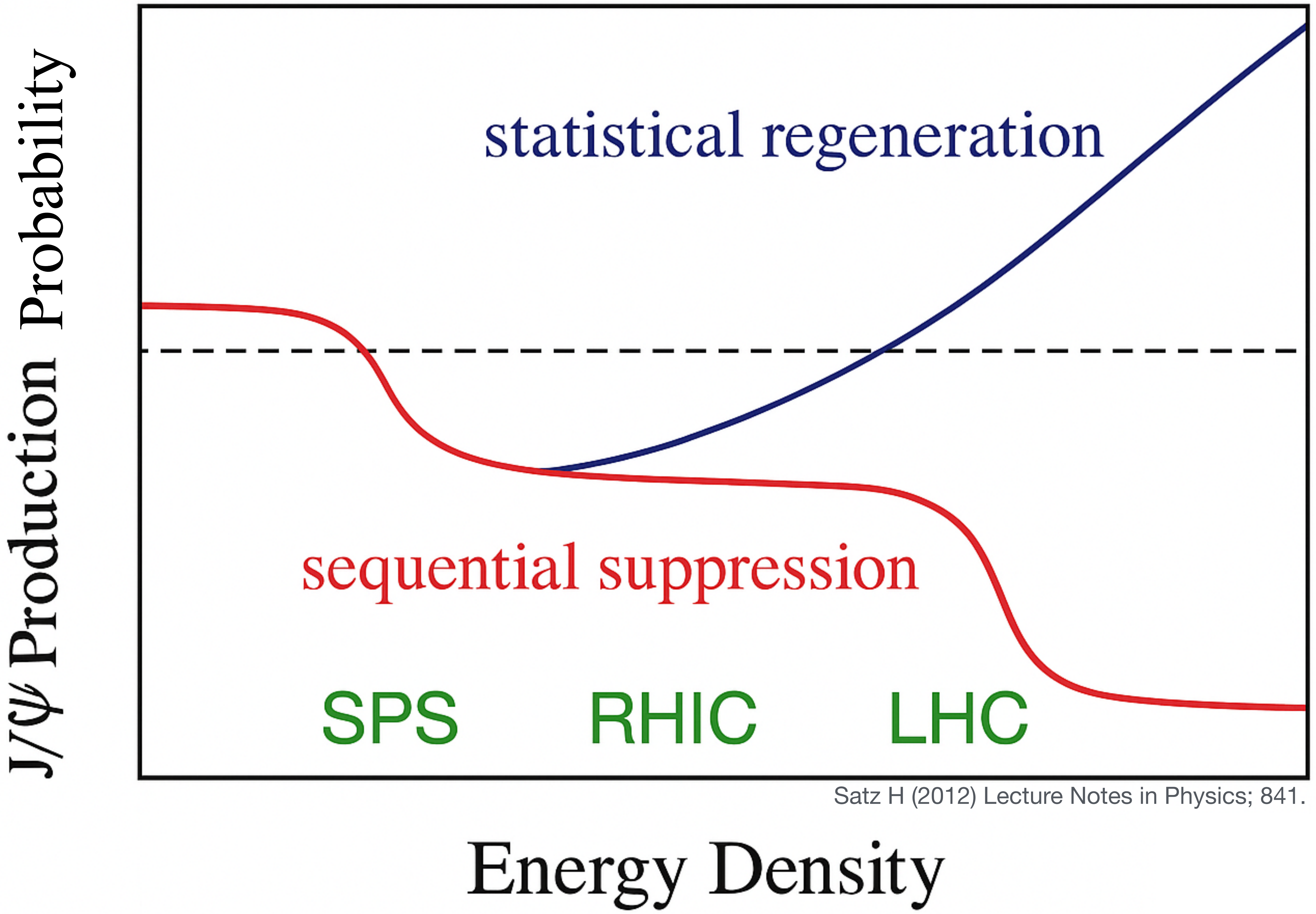

- **Dissociation** in QGP due to color screening:

➡ J/ψ suppression: signal for **deconfinement**

- At high energies: enhancement of charmonium yields due to **regeneration processes**

Modeling Heavy Quark Dynamics

Brownian Motion in the QGP

- Hierarchy of scales:

$$m_Q \gg T \text{ and } |\Delta\mathbf{p}| \ll |\mathbf{p}|$$

➡ multiple soft momentum transfers

- Leads to diffusive, stochastic motion: **Brownian dynamics**

- Basis for using **Langevin simulations**

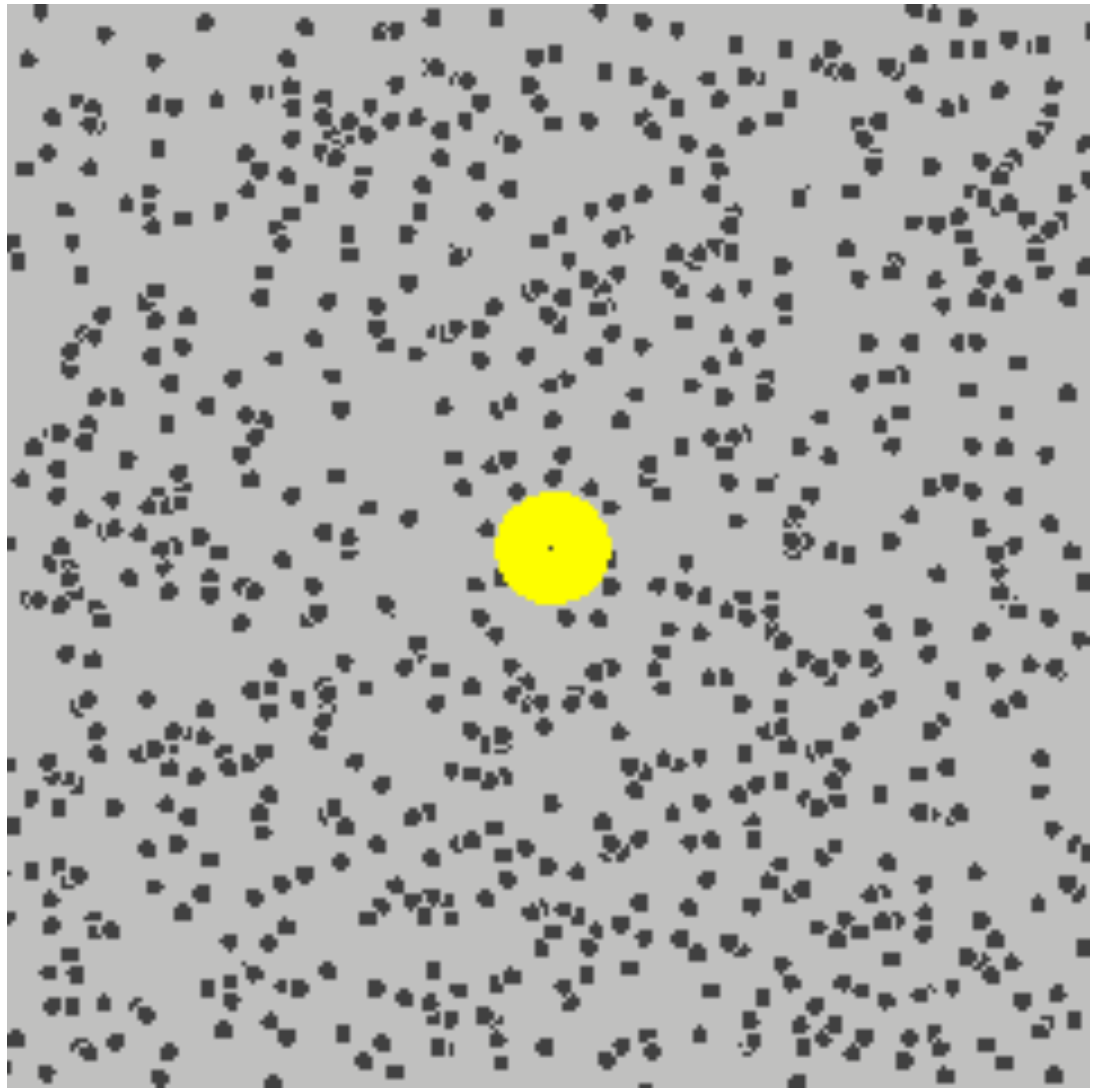

Modeling Heavy Quark Dynamics

Fokker Planck Equation

- Relativistic Boltzmann equation for heavy-quark phase-space distribution:

$$\left[\frac{\partial}{\partial t} + \frac{\boldsymbol{p}}{E}\frac{\partial}{\partial \boldsymbol{x}} + \boldsymbol{F}\frac{\partial}{\partial \boldsymbol{p}}\right] f_Q(t, p, x) = C[f_Q]$$

- Limit of small momentum exchanges $\rightarrow$ reduction to Fokker-Planck equation:

$$\frac{\partial}{\partial t} f_Q(\boldsymbol{p}, t) = \frac{\partial}{\partial p_i}\left\{A_i(\boldsymbol{p}) f_Q(\boldsymbol{p}, t) + \frac{\partial}{\partial p_j}[B_{ij}(\boldsymbol{p}) f_Q(\boldsymbol{p}, t)]\right\}$$

  - Drag: $A_i(\boldsymbol{p}, T) = A(\boldsymbol{p}, T) p_i \longrightarrow A(\boldsymbol{p}, T) \equiv \gamma(T)$
  - Diffusion: $B_{ij}(\boldsymbol{p}, T) = B_0(\boldsymbol{p}, T)\left(\delta_{ij} - \frac{p_i p_j}{p^2}\right) + B_1(\boldsymbol{p}, T)\frac{p_i p_j}{p^2}, \longrightarrow B_0(\boldsymbol{p}, T) = B_1(\boldsymbol{p}, T) \equiv D(\boldsymbol{p}, T)$

- Fluctuation-Dissipation Relation: $D[E(p)] = \gamma E(p) T$

Modeling Heavy Quark Dynamics

Langevin Dynamics

- Microscopical description: **Fokker-Planck → Langevin**

  ➡**Drag force (friction):** medium resistance

  ➡**Random noise (kicks):** thermal fluctuations

$$\frac{dp^\mu}{dt} = -\gamma p^\mu + \xi^\mu$$

- Corresponding update steps for coordinate and momentum in time step:

$$dx_j = \frac{p_j}{E} dt \ , \ dp_j = -\gamma p_j dt + \sqrt{2\gamma E T dt}\rho_j$$

➡Stochastic force ξ: gaussian white noise with $\langle \xi(t_1)\xi(t_2) \rangle = 2\gamma E T \delta(t_2 - t_1)$

Modeling Heavy Quark Dynamics

Langevin Dynamics

- So far: **free Brownian motion**
- Additional force to account for **bound-state formation**

➡ $V(r)$: potential between heavy quark and antiquark

➡ Complete momentum update step:

$$dp_j = -\gamma p_j dt + \sqrt{2\gamma ETdt}\rho_j - \nabla_j V(r)dt$$

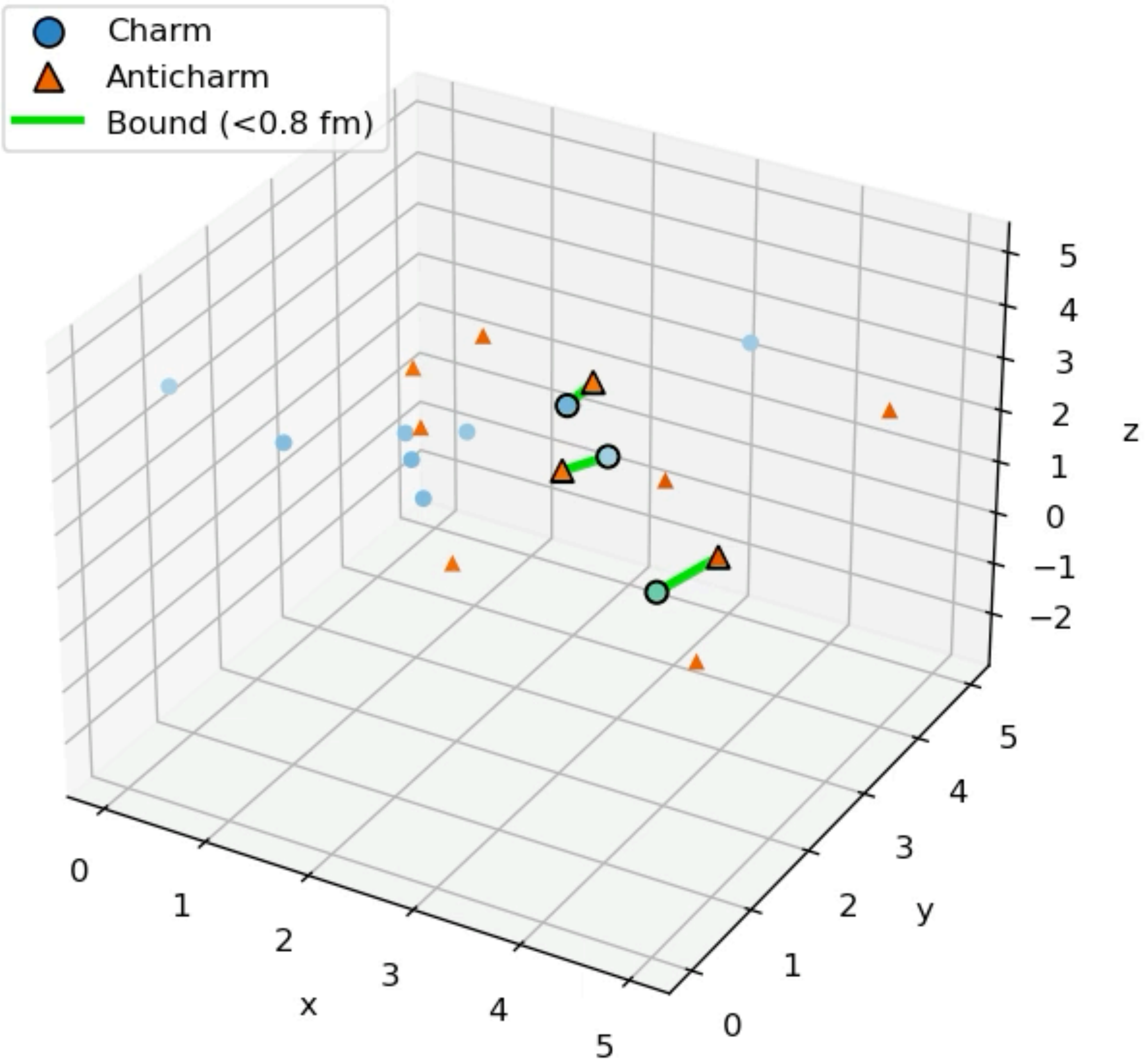

➡ Time evolution of microscopic trajectories of heavy quarks and quarkonium

Complex Potential

Bound State Formation

- In-medium interaction between a heavy quark and antiquark described by complex potential:

$$\mathscr{V}(r) = \mathrm{Re}[\mathscr{V}(r)] + i\,\mathrm{Im}[\mathscr{V}(r)]$$

$$\mathrm{Re}[\mathscr{V}(r)] = V(r) = -\frac{g^2}{4\pi}m_D - \frac{g^2}{4\pi}\frac{\exp(-m_D r)}{r}$$

➡screened binding

Blaizot et al., Nucl.Phys.*A* 946 (2016) 49-88

$$\mathrm{Im}[\mathscr{V}(r)] = -\frac{g^2 T}{4\pi}\phi(m_D r)$$

➡in-medium dissociation rate

Laine et al., JHEP03 (2007) 054

Complex Potential: Real Part

Bound State Formation

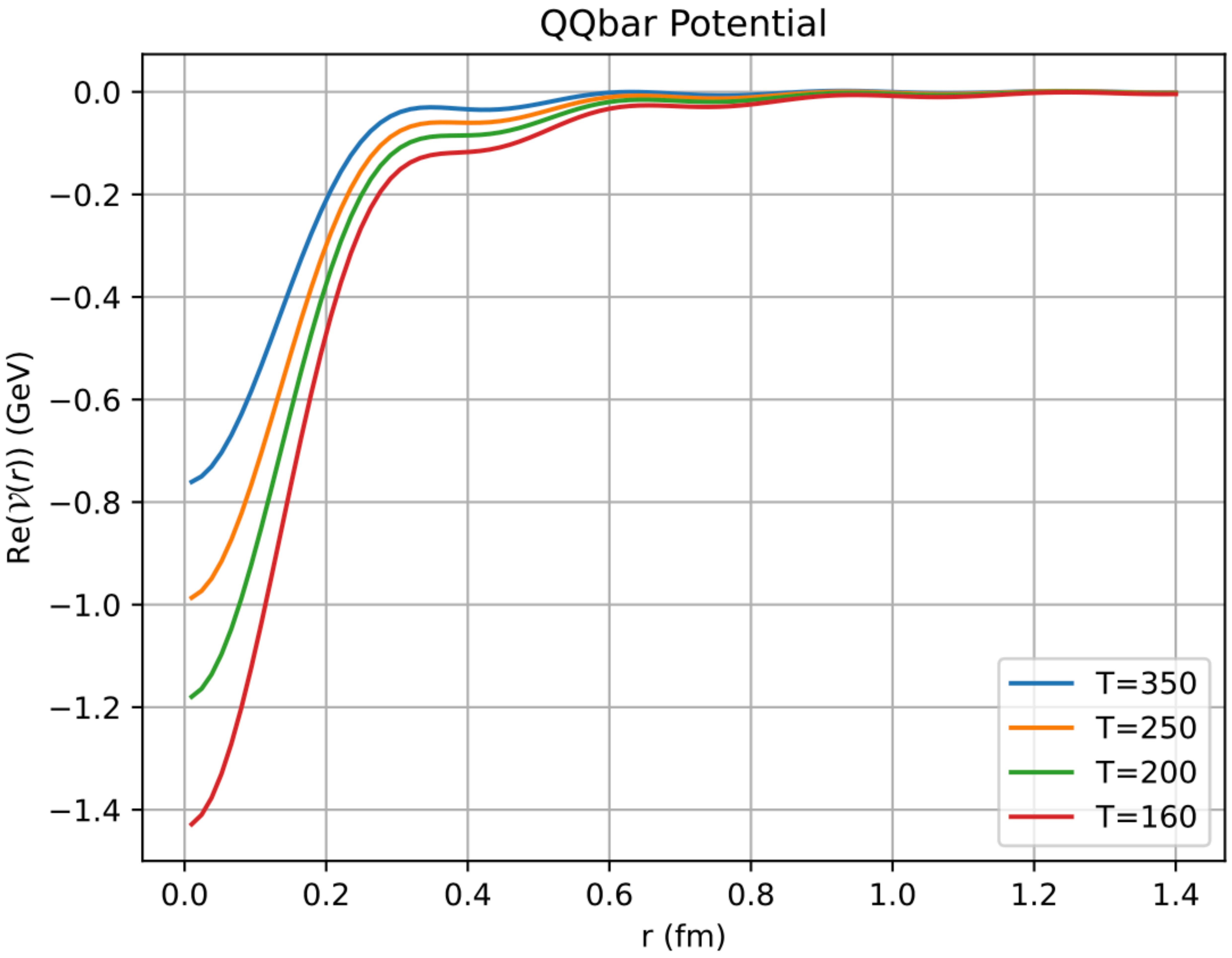

- Running coupling:

$$g^2 = 4\pi\alpha_s = \frac{4\pi\alpha_s(T_c)}{1 + 0.76\ \ln(T/T_c)},$$

Blaizot et al., Nucl.Phys.*A* 946 (2016) 49-88

$$\alpha_s(T_c) = 0.7$$

- Screening effects at higher temperatures

➡Fraction of bound state decreases

Complex Potential: Imaginary Part

Drag & Diffusion Coefficient

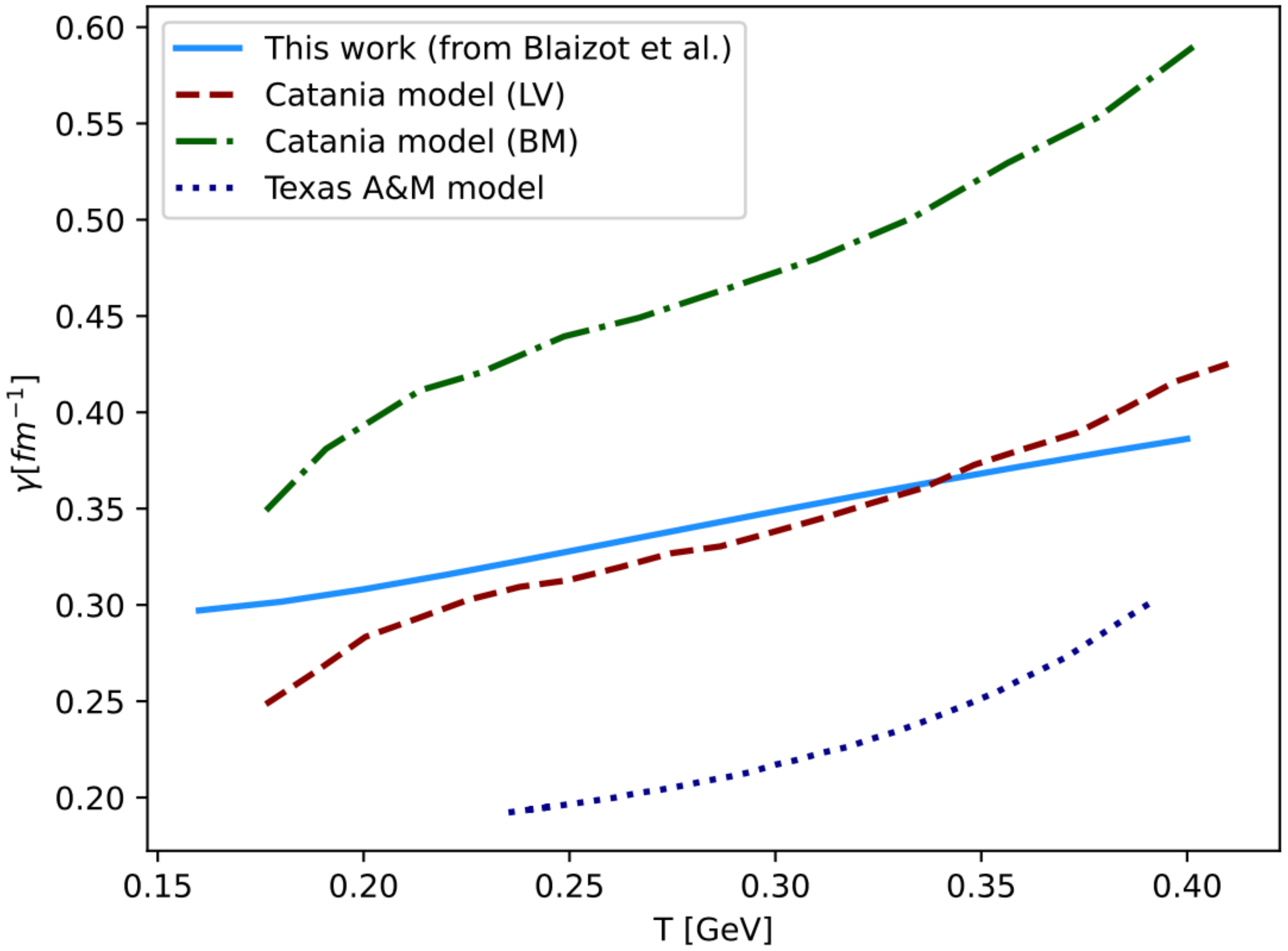

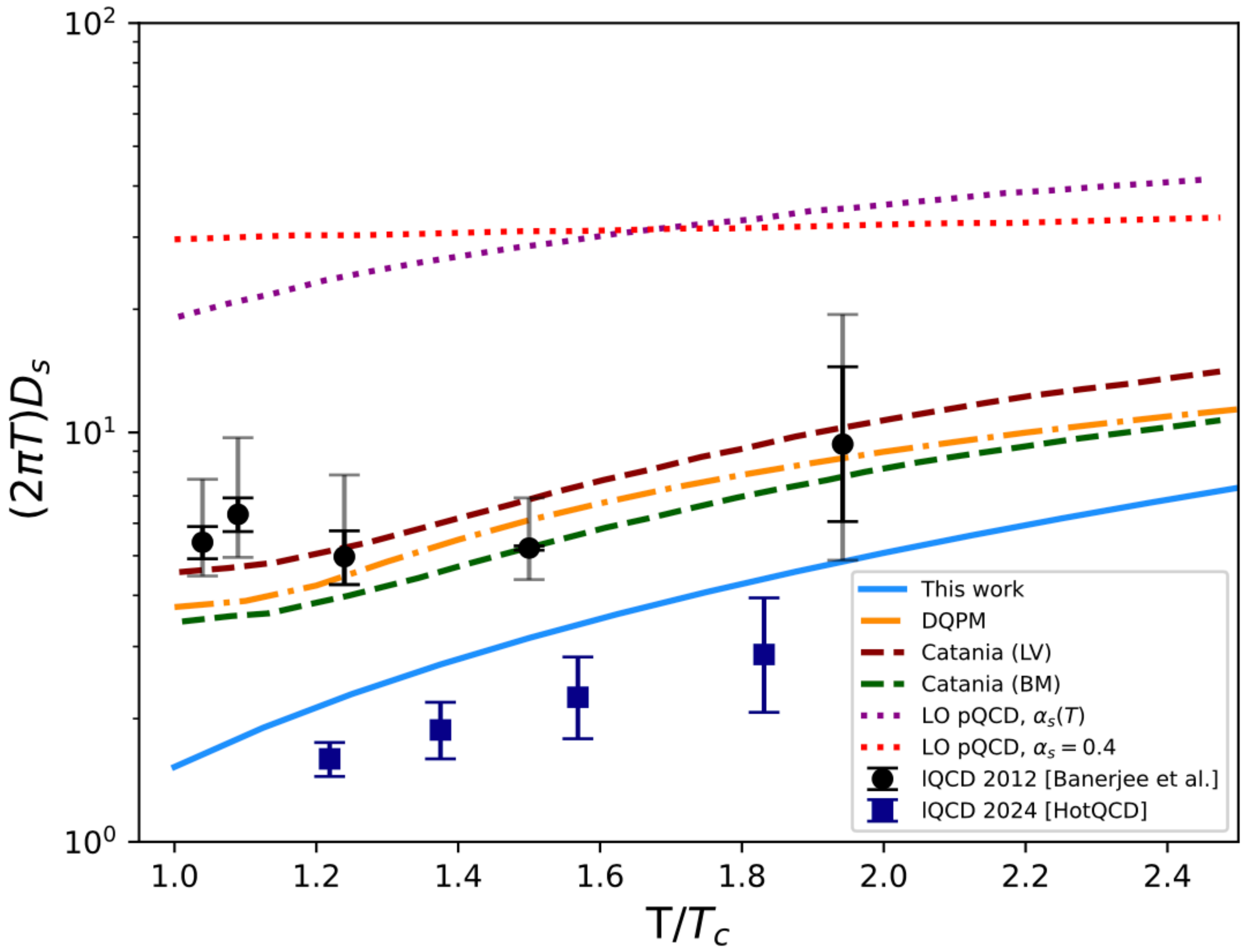

From $\mathrm{Im}[\mathscr{V}(r)]$:

$$\gamma = \frac{m_D^2}{24\pi M}\left[\ln\left(1+\frac{\Lambda^2}{m_D^2}\right) - \frac{\Lambda^2/m_D^2}{1+\Lambda^2/m_D^2}\right] \quad \longrightarrow \quad D_s = \frac{T}{M_c\gamma}, \qquad M_c = 1.8\ \mathrm{GeV/c^2}$$

Blaizot et al., Nucl.Phys.*A* 946 (2016) 49-88

Equilibration & Bound State Formation

Box Simulations at fixed T and V

Equilibrated distribution of relative energy of charm-anticharm pairs:

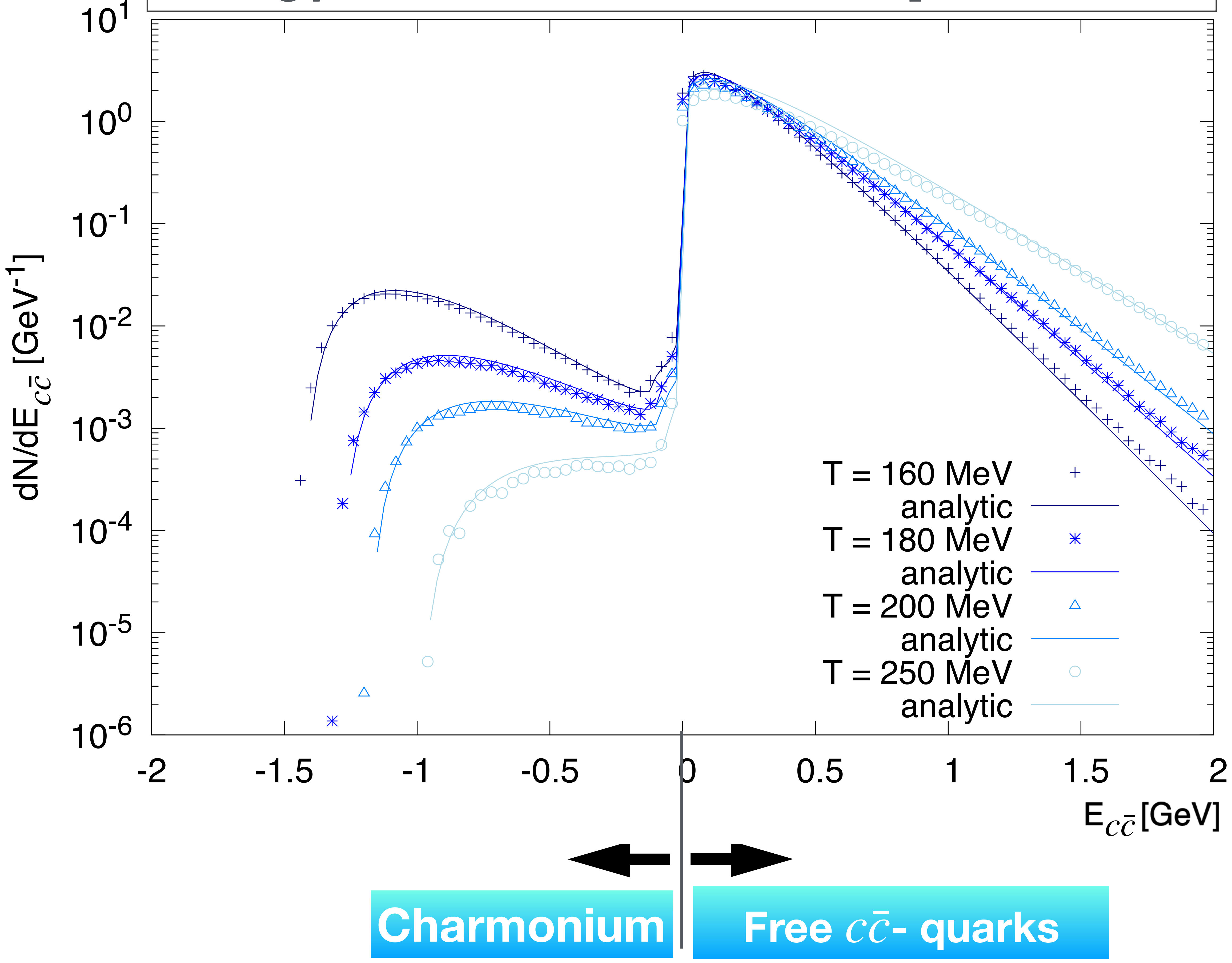

Criterion for bound state formation:

$$E_{c\bar{c}} = E_c + E_{\bar{c}} + V(|\boldsymbol{r}_c - \boldsymbol{r}_{\bar{c}}|) - E_{cm} < 0$$

$$= \sqrt{m_c^2 + \mathbf{p_c^2}} + \sqrt{m_{\bar{c}}^2 + \mathbf{p_{\bar{c}}^2}} + V(|\mathbf{r_c} - \mathbf{r_{\bar{c}}}|) - \sqrt{(\mathbf{m_c} + \mathbf{m_{\bar{c}}})^2 + (\mathbf{p_c} + \mathbf{c_{\bar{c}}})^2} < \mathbf{0}$$

Energy distribution in equilibrium:

$$\frac{dN}{dE_{c\bar{c}}} = (4\pi)^2 (2\mu)^{\frac{3}{2}} C \int_0^R drr^2 \sqrt{E_{c\bar{c}} - V(r)} \exp\left(-\frac{E_{c\bar{c}}}{T}\right)$$

➡ Simulation leads to correct equilibrium density of states

Binding Length of Charmonium

Probability distribution of the relative distance

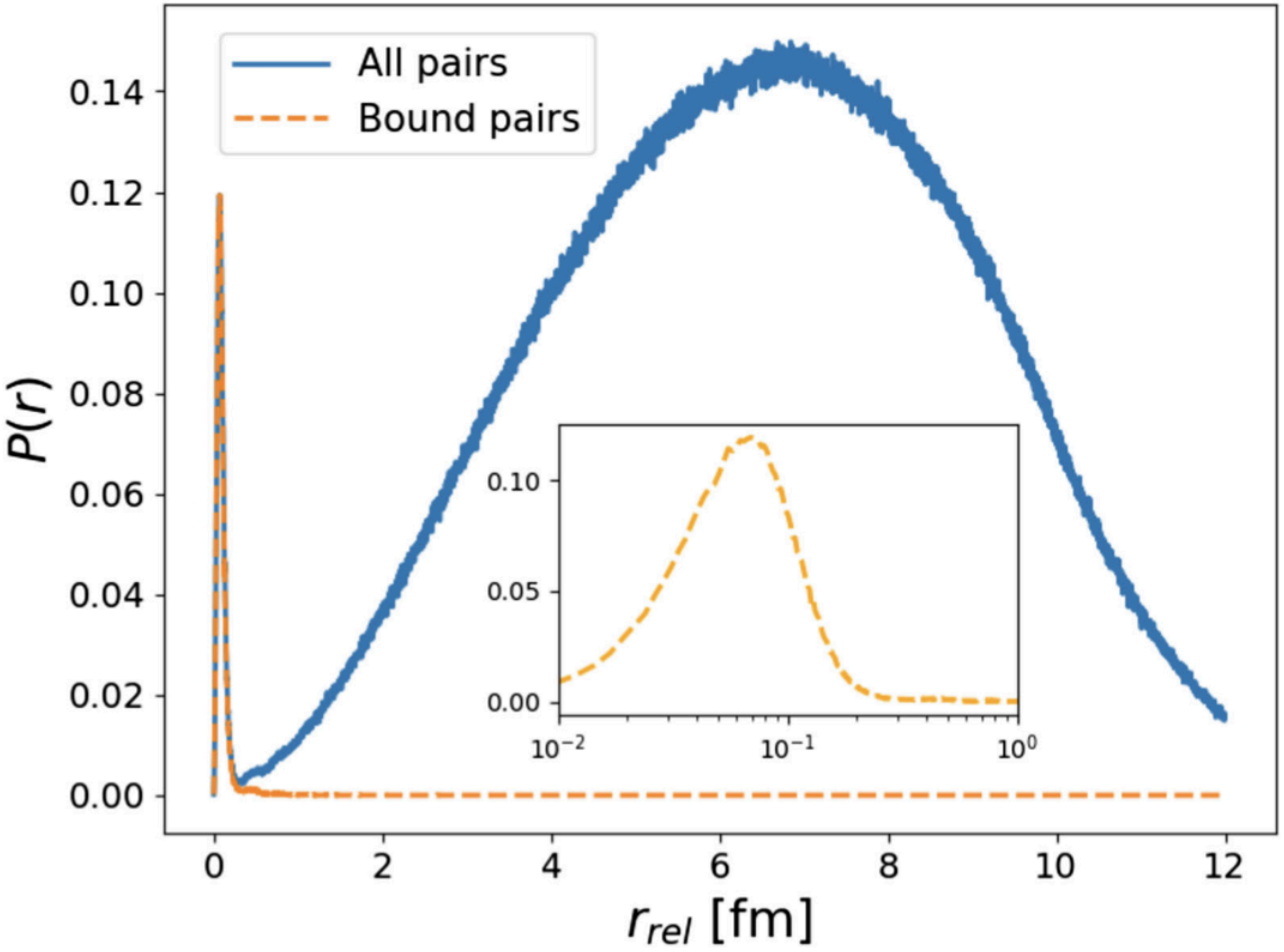

- peak at small distances: relative distance within a bound state
- larger distances: potential becomes negligible
- distance distribution depending on the box size (second peak)

Equilibration & Bound State Formation

Box Simulations at fixed $T = 180\ \mathrm{MeV}$ and V

Time evolution of bound state formation:

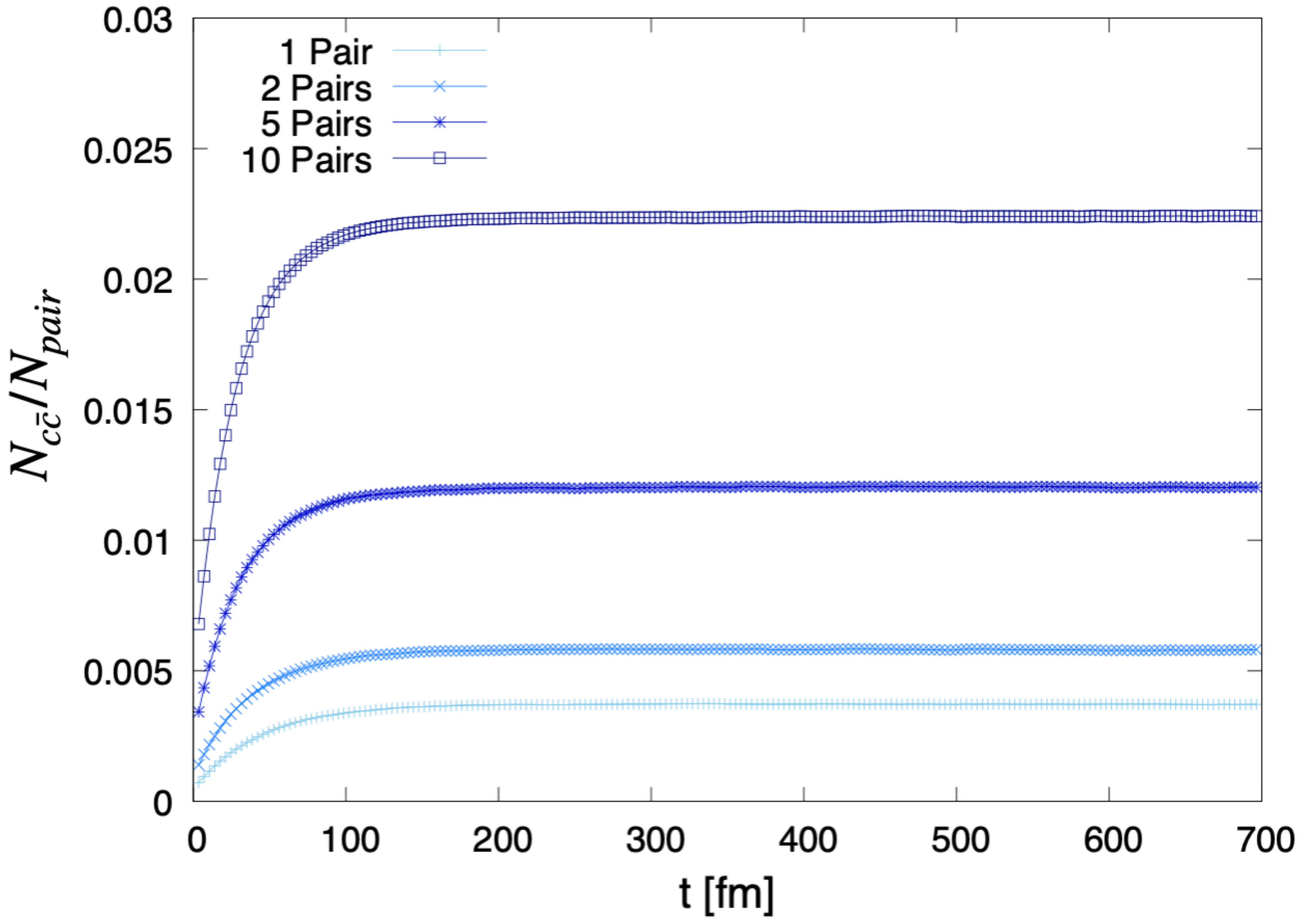

Equilibration & Bound State Formation

Box Simulations at fixed T and V

Time evolution of bound state formation:

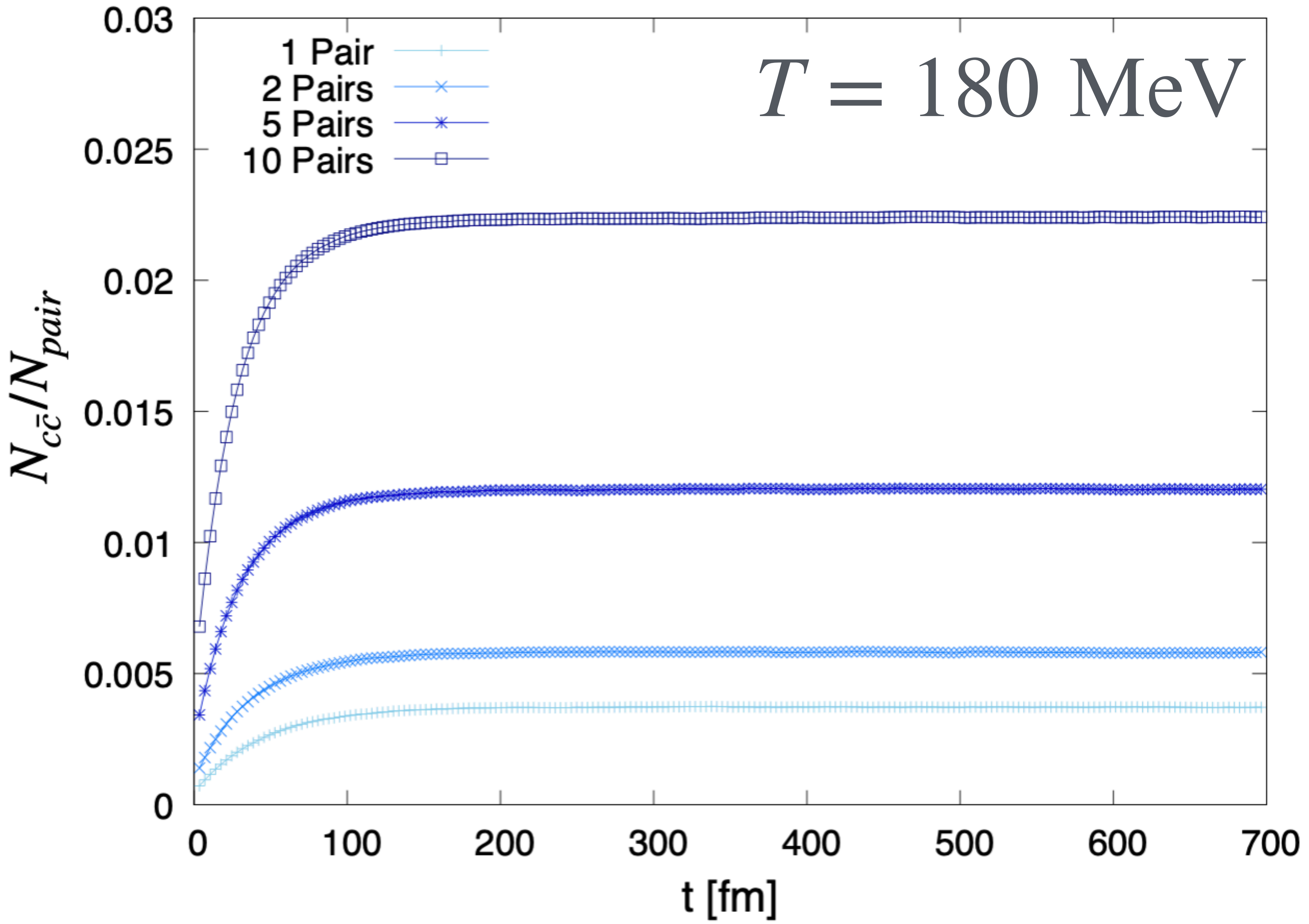

Initially free vs. initially bound pairs:

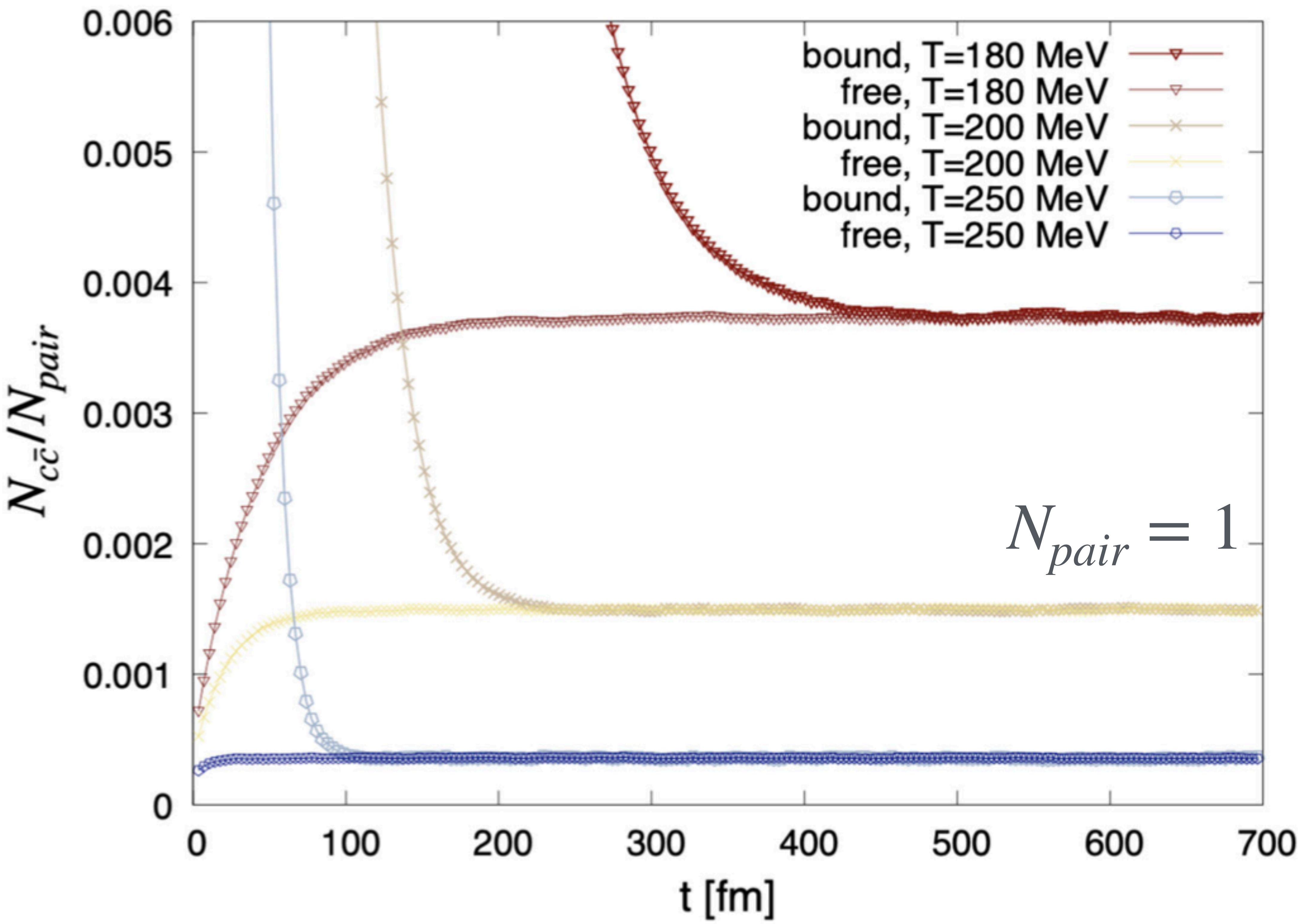

➡Detailed balance between dissociation and regeneration processes

Equilibration & Bound State Formation

Time evolution of fraction of bound states in Box Simulations

Different Volumes $N_{pairs} = 1, \ T = 180 \text{ MeV}$

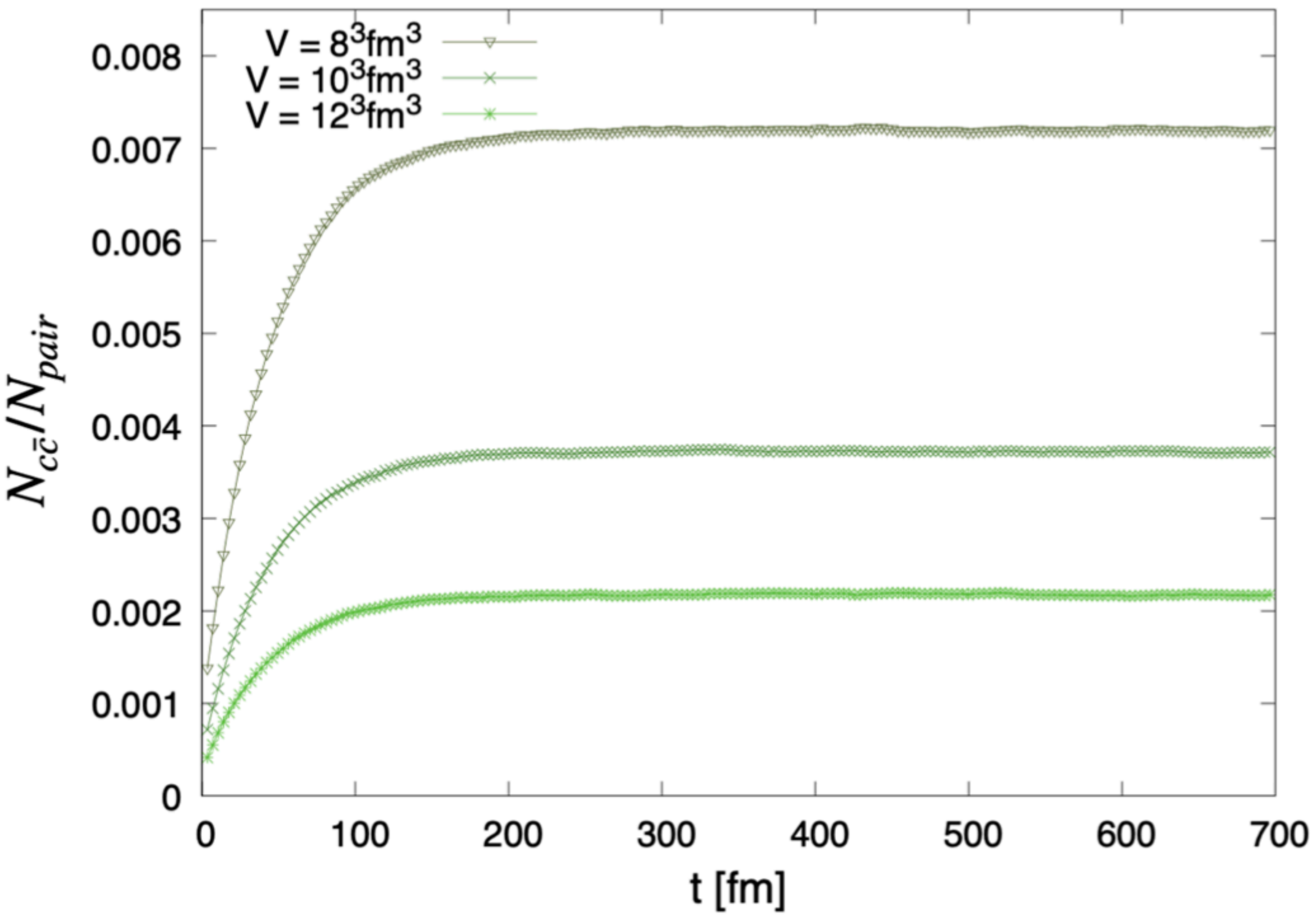

Different Temperatures, $N_{pairs} = 1$

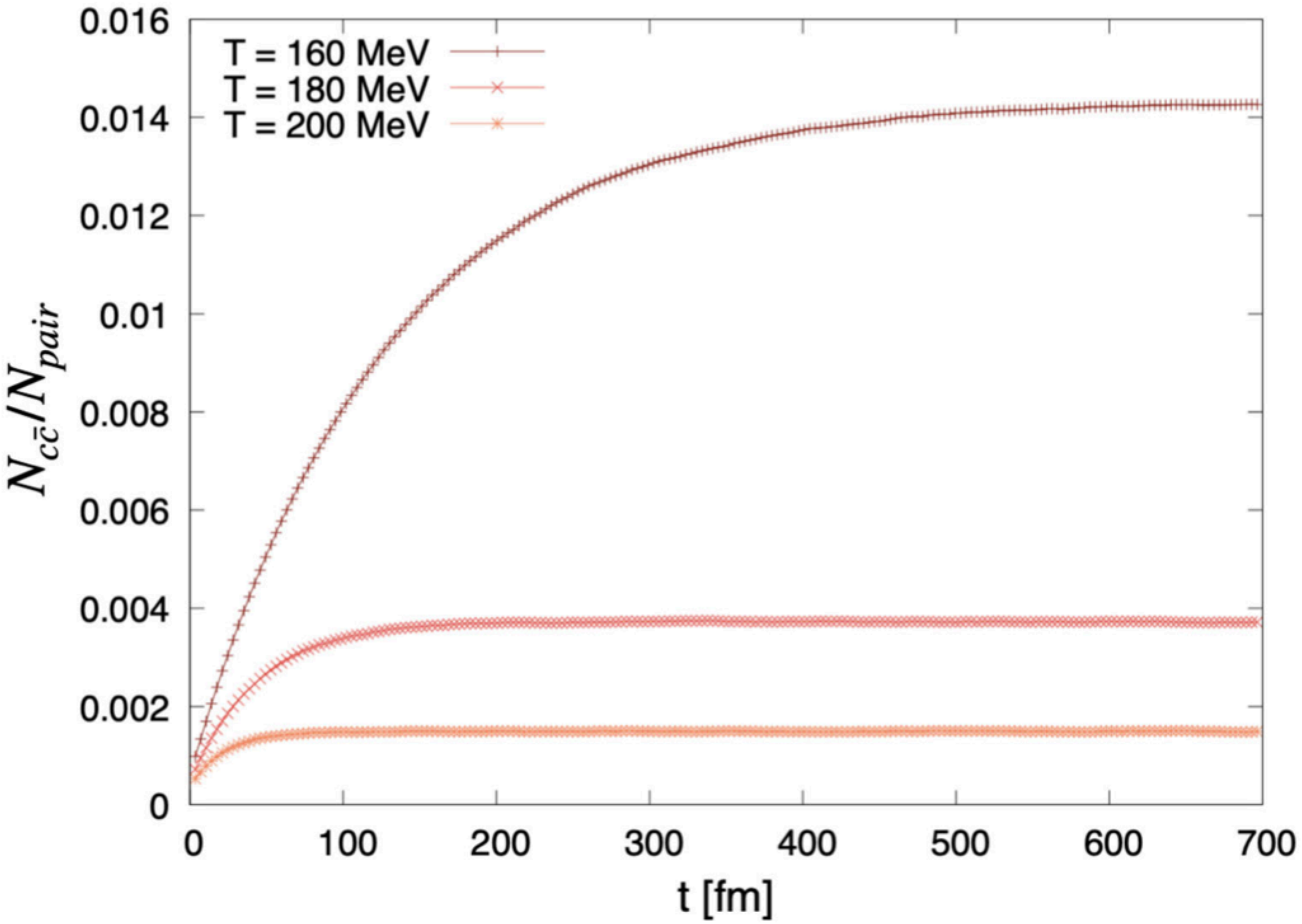

Equilibration time

Different scalings of drag coefficient γ ($T = 160$ MeV)

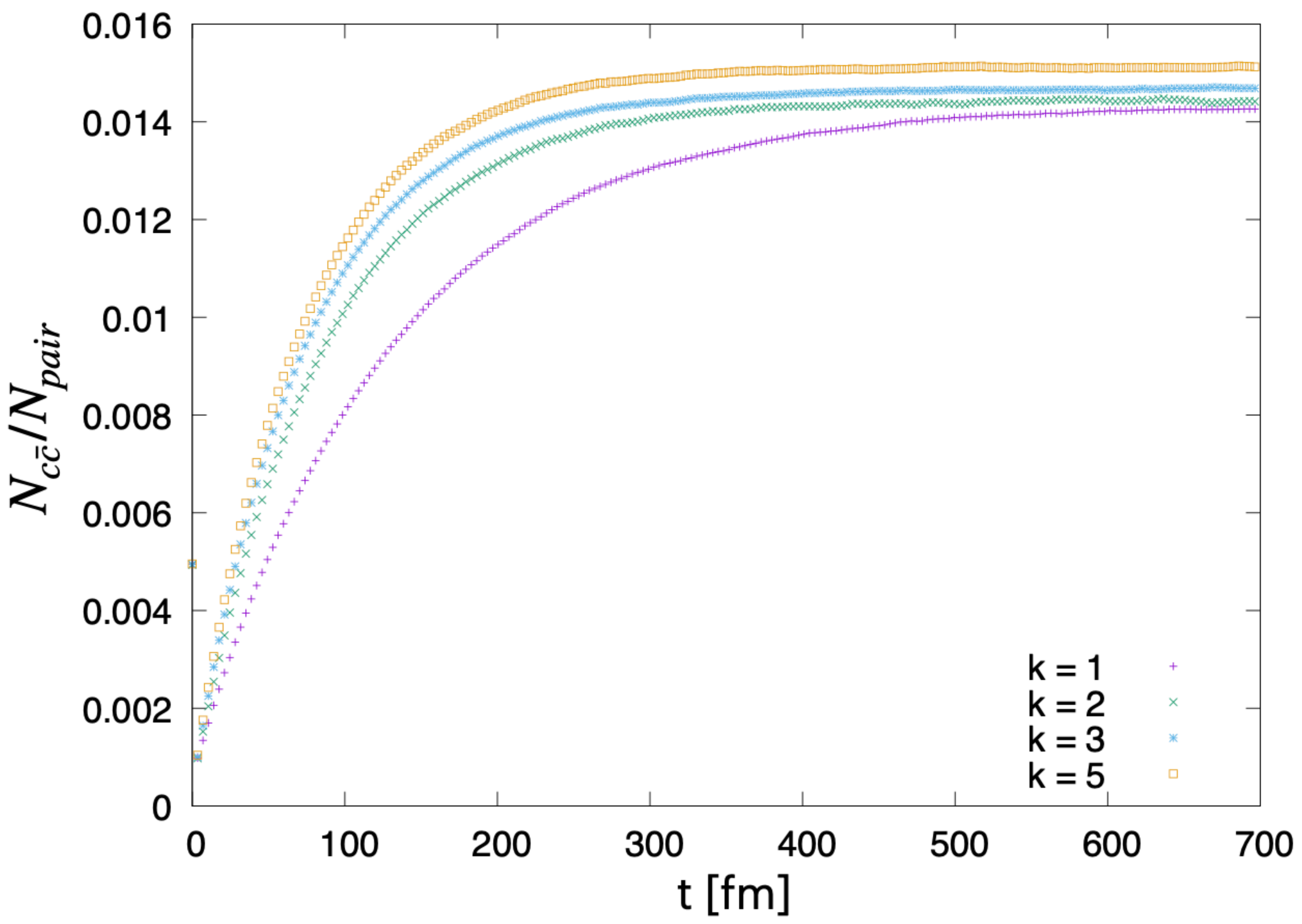

- Faster equilibration for stronger drag force
- 2 intertwined mechanisms:
  1. Charm momentum relaxation towards thermal value: $\tau_{eq} = 1/\gamma$
  2. Full equilibration = time-independent number of bound states

     ➡ dominated by time scales of the potential

Modelling the QGP Medium

Elliptic Blast-Wave Fireball

H. van Hees, M. He, and R. Rapp, Nuclear Physics A, (2015) Vol. 933

- Elliptic parametrisation of transverse direction:

$$\frac{x^2}{b^2(\tau)} + \frac{y^2}{a^2(\tau)} \leq 1$$

- **Transverse flow:** encoded via time-dependent semi-axes

$$a(\tau) = a_0 + \frac{1}{a_a}\left(\sqrt{1 + {a_a}^2\tau^2} - 1\right),\; b(\tau) = b_0 + \frac{1}{a_b}\left(\sqrt{1 + {a_b}^2\tau^2} - 1\right)$$

- a_a, a_b: accelerations chosen to fit to p_T-spectra and elliptic flow of light hadrons

- **Longitudinal direction:** boost-invariant Bjorken flow, $v_z = \frac{z}{t}$

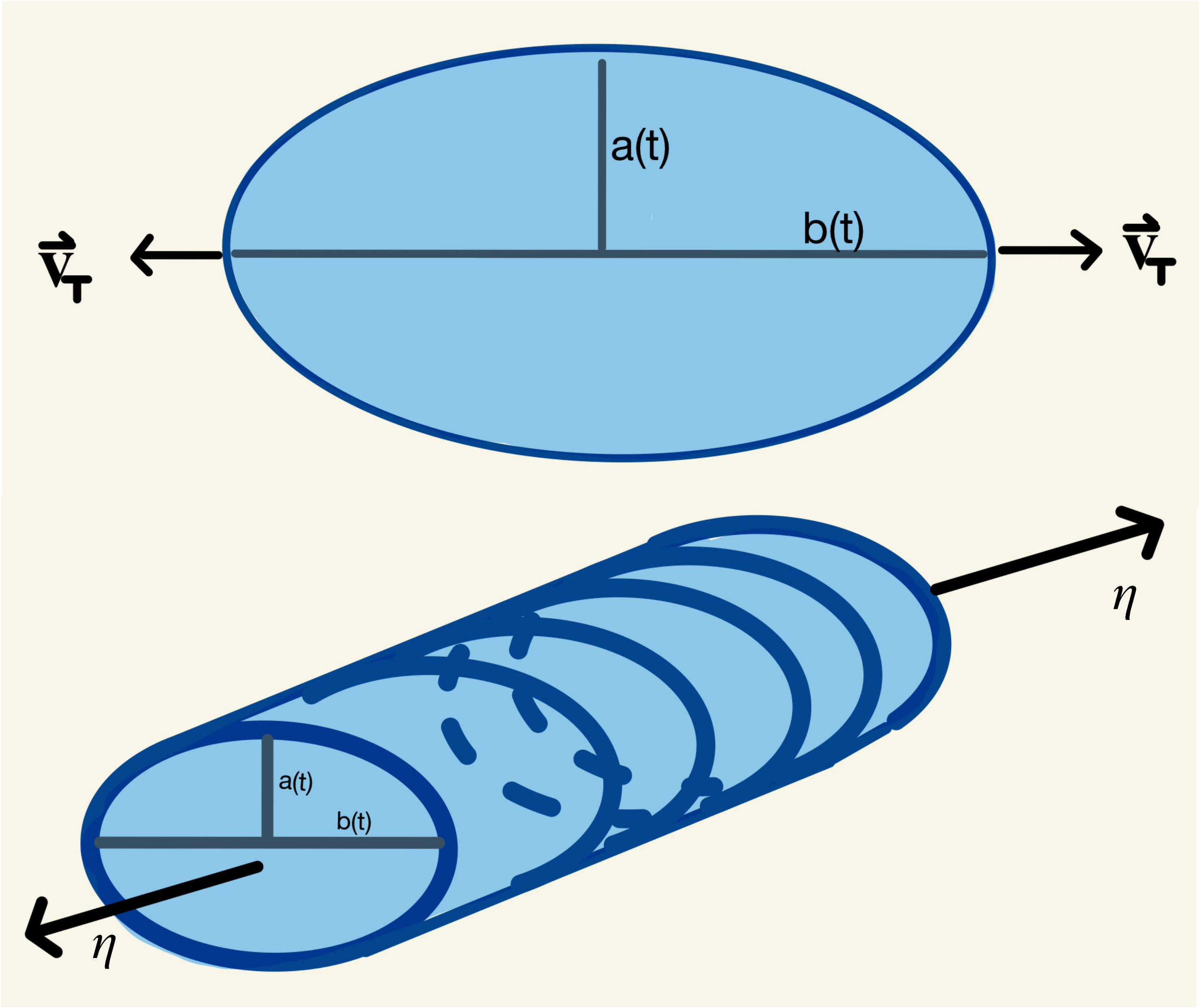

Modelling the QGP Medium

Elliptic Blast-Wave Fireball

- 3D-flow field:

$$v_x = \frac{\tau}{t} v_b(\tau) \cos(v) \frac{r}{r_B}, \; v_y = \frac{\tau}{t} v_a(\tau) \sin(v) \frac{r}{r_B}, \; v_z = \tanh(\eta)$$

- Parametrization of different energies and centrality classes:

LHC@2.76 TeV, 0-20% | LHC@2.76 TeV, 20-40%

RHIC@200 GeV, 20-40%

- Initial momentum distribution: PYTHIA
- Initial spatial distribution: Glauber model

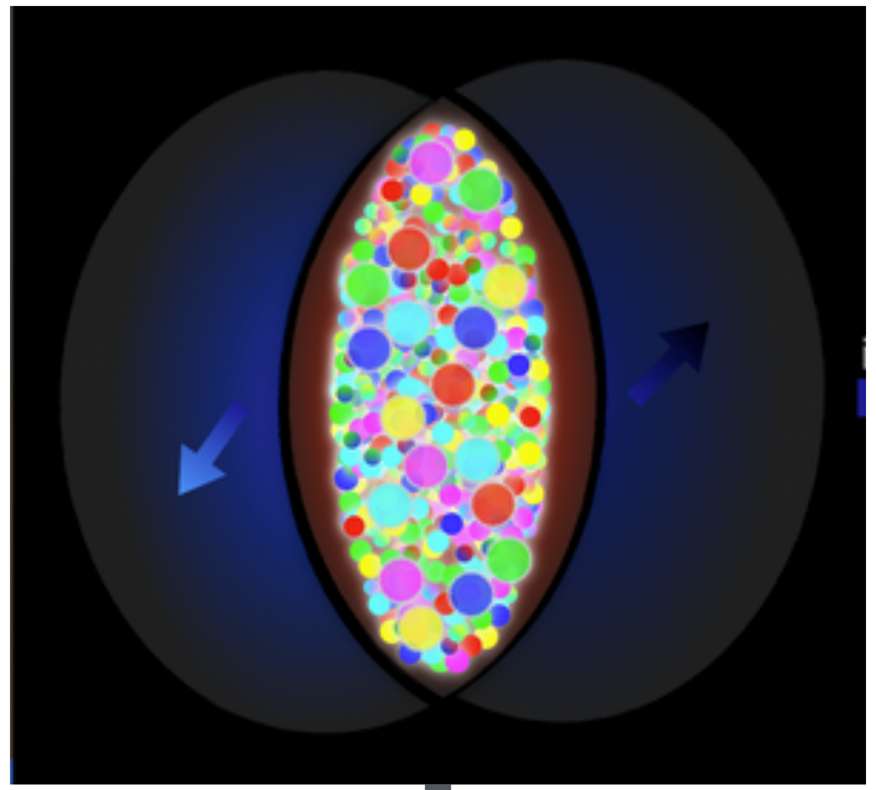

https://irfu.cea.fr/dap/en/Phocea/Vie_des_labos/Ast/ast.php?t=fait_marquant&id_ast=4733

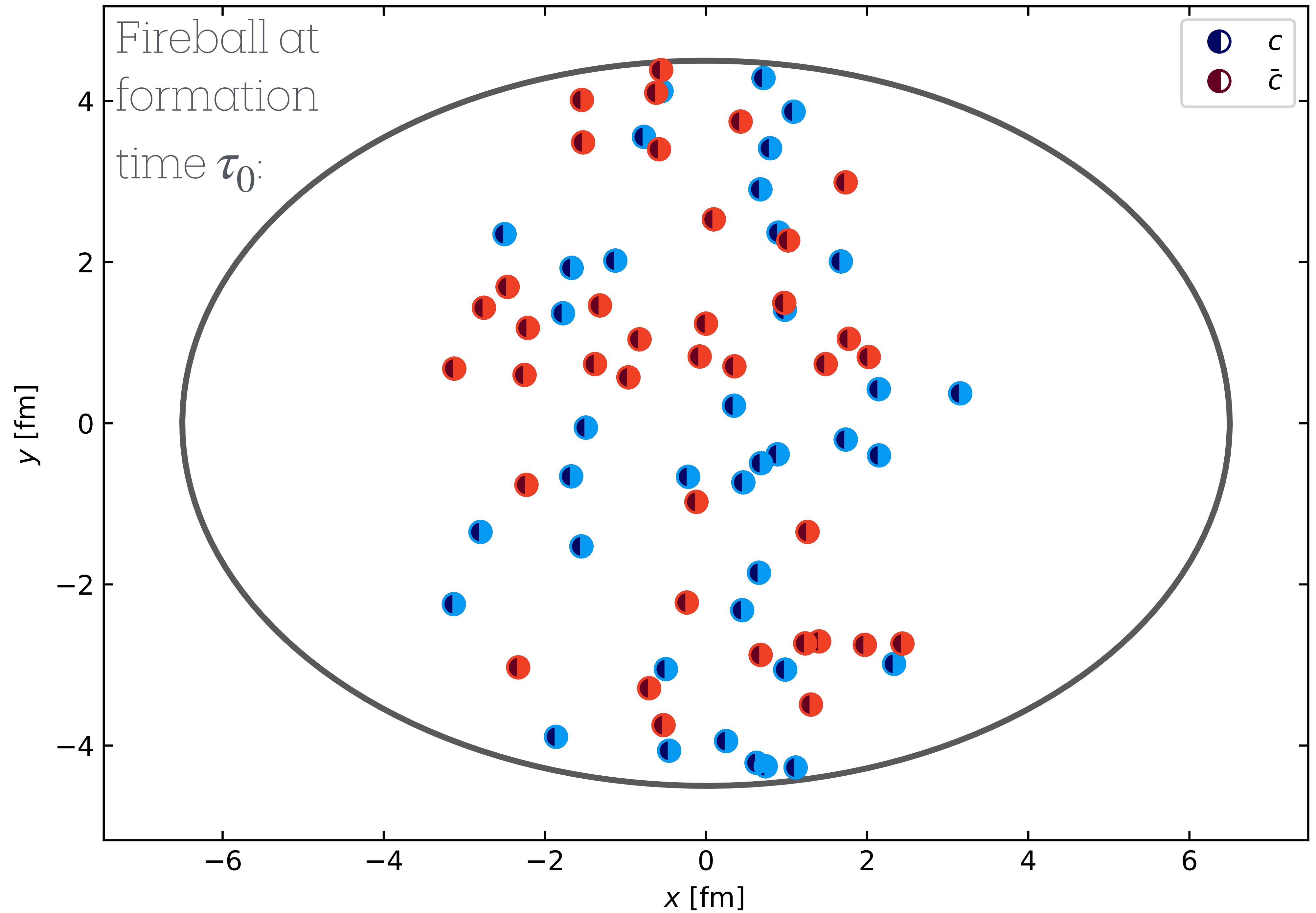

Number of produced charm-anticharm pairs $N_{c\bar{c}}$

Estimation from Glauber model

- Number of charm quark pairs per rapidity:

$$\frac{dN_{c\bar{c}}}{dy} = T_{AA}(b)\frac{d\sigma_{c\bar{c}}^{pp}}{dy} = T_{AA}(b)\ \sigma_{c\bar{c}}^{pp}\frac{dN_{c\bar{c}}^{pp}}{dy}$$

- Overlap function:

$$T_{AA}(b) = \int_{-\infty}^{\infty} ds^2 T_A(\boldsymbol{s}) T_B(\boldsymbol{s}-\boldsymbol{b})$$

with $T_A(\boldsymbol{s}) = \int \rho_A(\boldsymbol{s},\boldsymbol{z})dz$ and $\rho_A(r) = \dfrac{\rho_0}{1+\exp\left(\frac{r-r_0}{a}\right)}$

Number of produced charm-anticharm pairs $N_{c\bar{c}}$

Estimation from Glauber model

- Number of charm quark pairs per rapidity:

$$\frac{dN_{c\bar{c}}}{dy} = T_{AA}(b)\frac{d\sigma_{c\bar{c}}^{pp}}{dy} = T_{AA}(b)\ \sigma_{c\bar{c}}^{pp}\frac{dN_{c\bar{c}}^{pp}}{dy}$$

- Overlap function:

$$T_{AA}(b) = \int_{-\infty}^{\infty} ds^2 T_A(\boldsymbol{s}) T_B(\boldsymbol{s} - \boldsymbol{b})$$

with $T_A(\boldsymbol{s}) = \int \rho_A(\boldsymbol{s}, z) dz$ and $\rho_A(r) = \dfrac{\rho_0}{1 + \exp\left(\frac{r - r_0}{a}\right)}$

➡Experimental data from pp collisions

➡Obtained from Pythia

➡Parameters of nuclei

Number of produced charm-anticharm pairs $N_{c\bar{c}}$

Estimation from Glauber model

$$\frac{dN_{c\bar{c}}}{dy} = T_{AA}(b)\frac{d\sigma^{pp}_{c\bar{c}}}{dy} = T_{AA}(b)\ \sigma^{pp}_{c\bar{c}}\frac{dN^{pp}_{c\bar{c}}}{dy}$$

- Overlap function $T_{AA}(b) = \int_{-\infty}^{\infty} ds^2 T_A(\mathbf{s})T_B(\mathbf{s}-\mathbf{b})$

with $T_A(\mathbf{s}) = \int \rho_A(\mathbf{s}, z)dz$ and $\rho_A(r) = \dfrac{\rho_0}{1+\exp\left(\frac{r-r_0}{a}\right)}$

➡ Number of produced charm quarks:

	b [fm]	$N_{c\bar{c}}$
RHIC (20-40%)	8.05	4
LHC (0-20%)	3.976	105
LHC (20-40%)	8.43	38

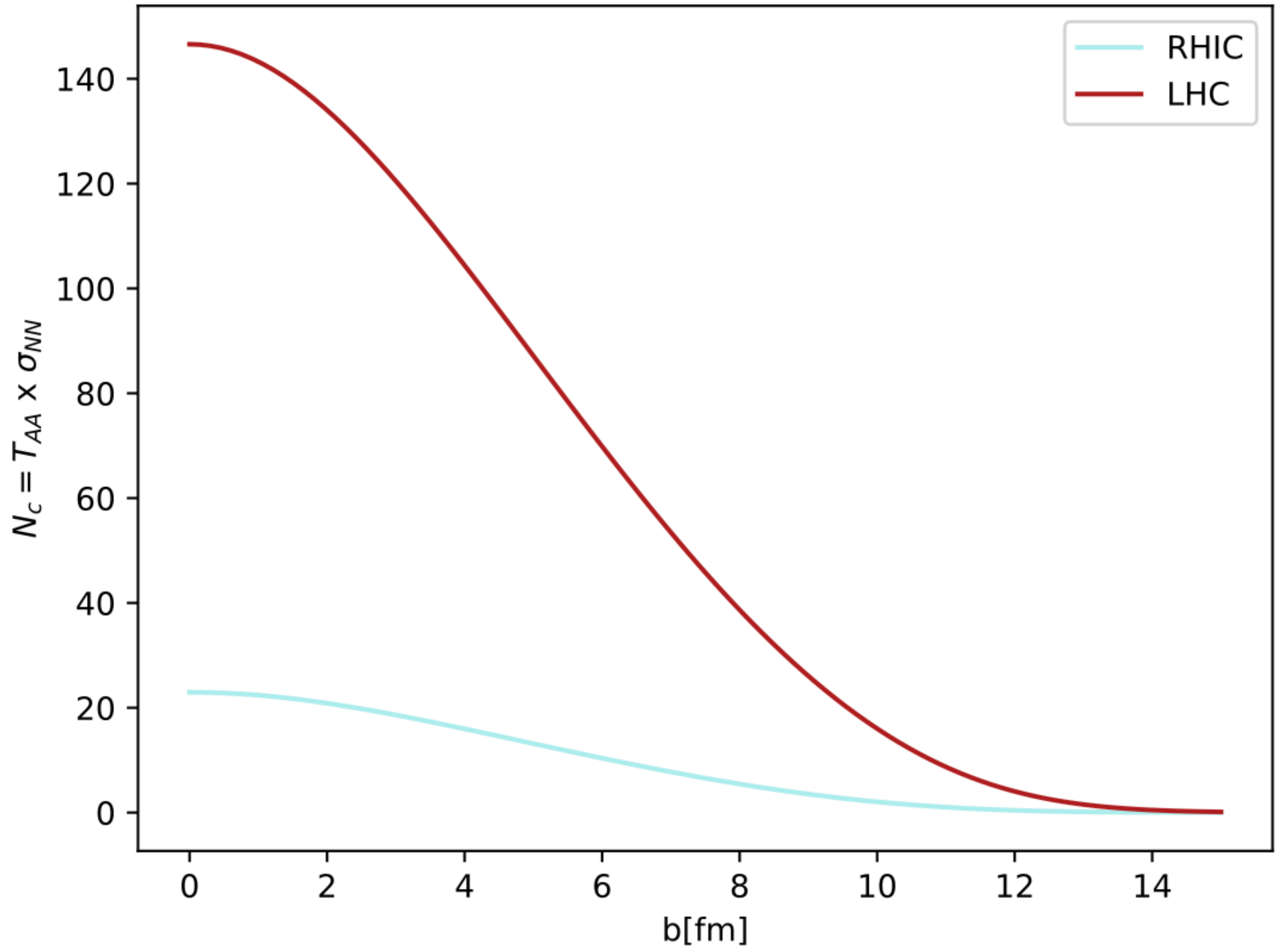

J/ψ - Production

Differential yield per rapidity $dN_{J/\psi}/dy$ at T_{ch}

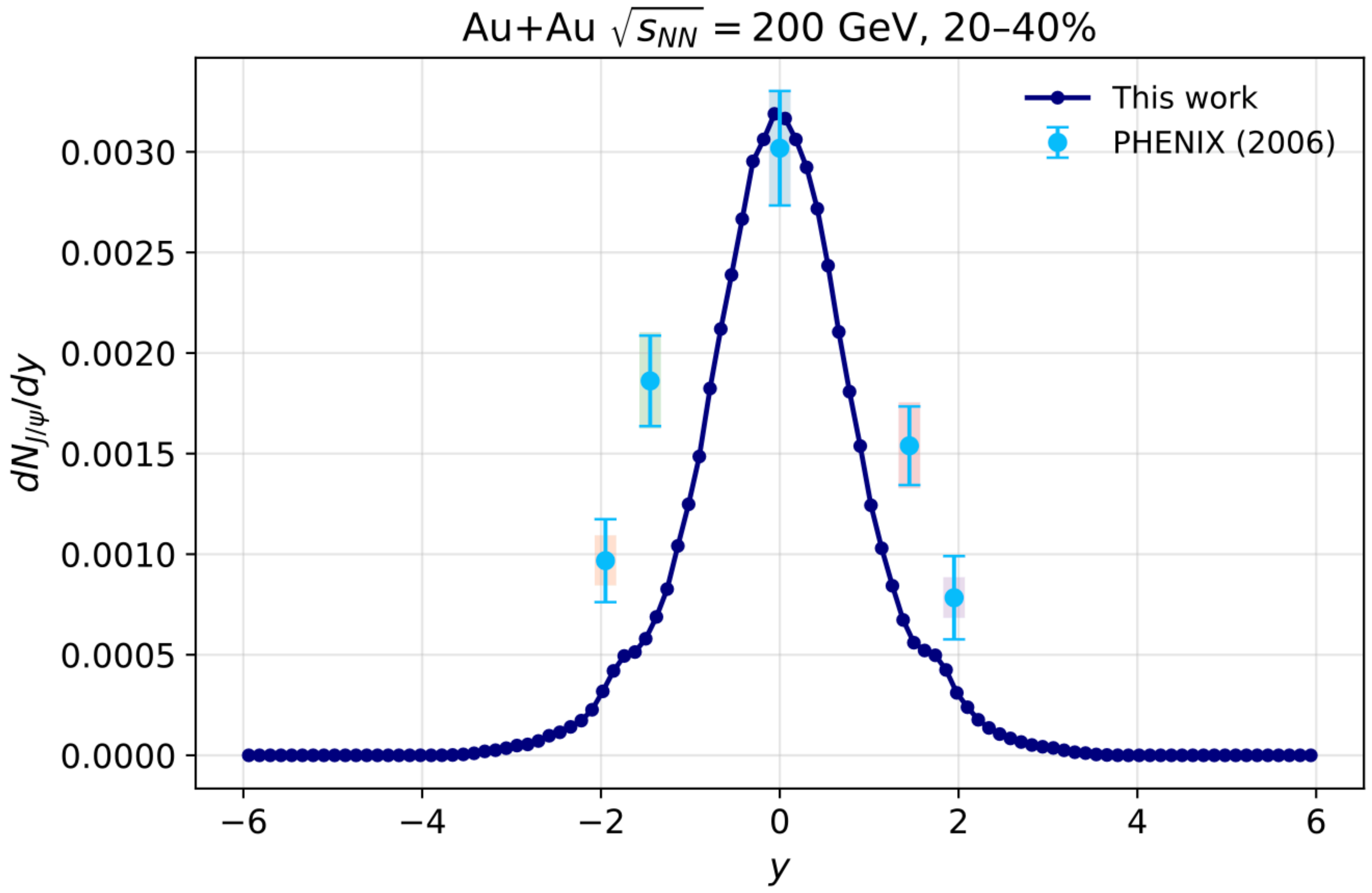

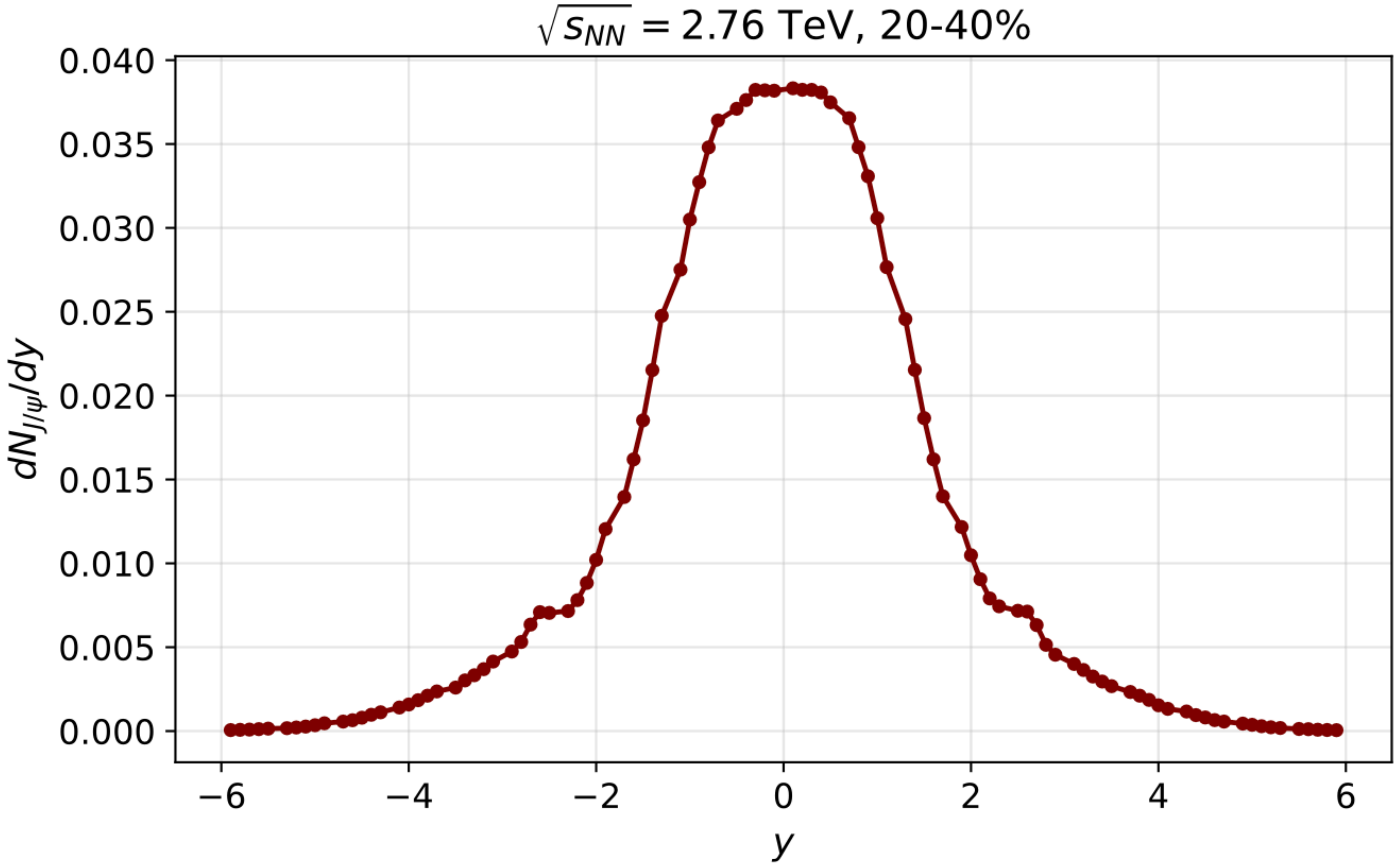

PHENIX Collaboration (2006). J/Psi production vs Centrality, Transverse Momentum, and Rapidity in Au+Au Collisions at in Au Au collisions at $\sqrt{s_{NN}}$ = 200 GeV. *Phys.Rev.Lett.* 98 (2007) 232301

$$\frac{dN_{J/\psi}}{dy}\Big|_{y=0} = 0.0032$$

$$\frac{dN_{J/\psi}}{dy}\Big|_{y=0} = 0.0379$$

Charm Elliptic Flow v_2

Au+Au @ 200 GeV and Pb+Pb @ 2.76 TeV

Charm-quark v_2 at midrapidity: Energy dependence

$$v_2 = \left\langle \frac{p_x^2 - p_y^2}{p_x^2 + p_y^2} \right\rangle$$

Time evolution of v_2 at $\sqrt{s_{NN}} = 2.76$ TeV, 20-40% centrality

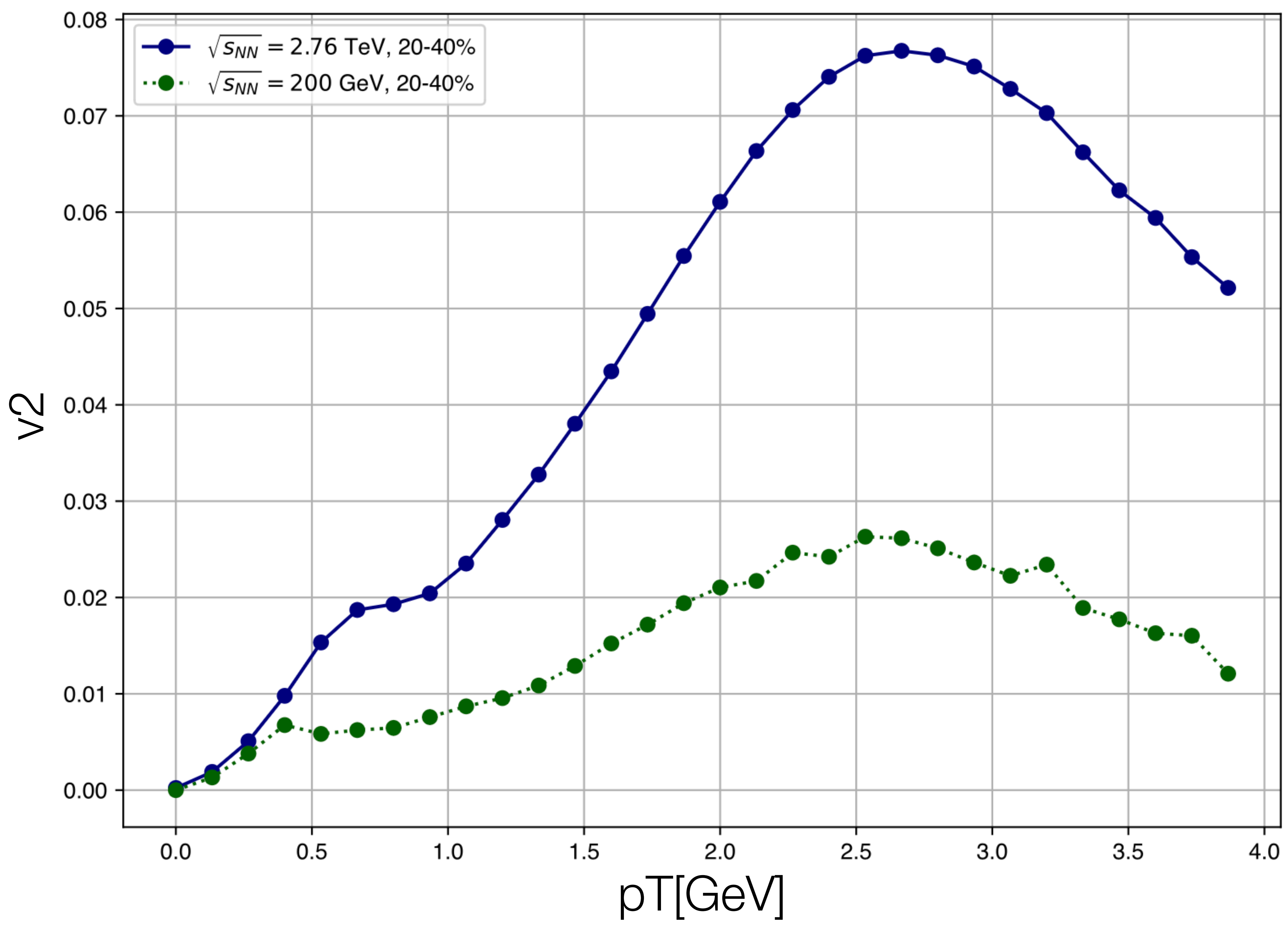

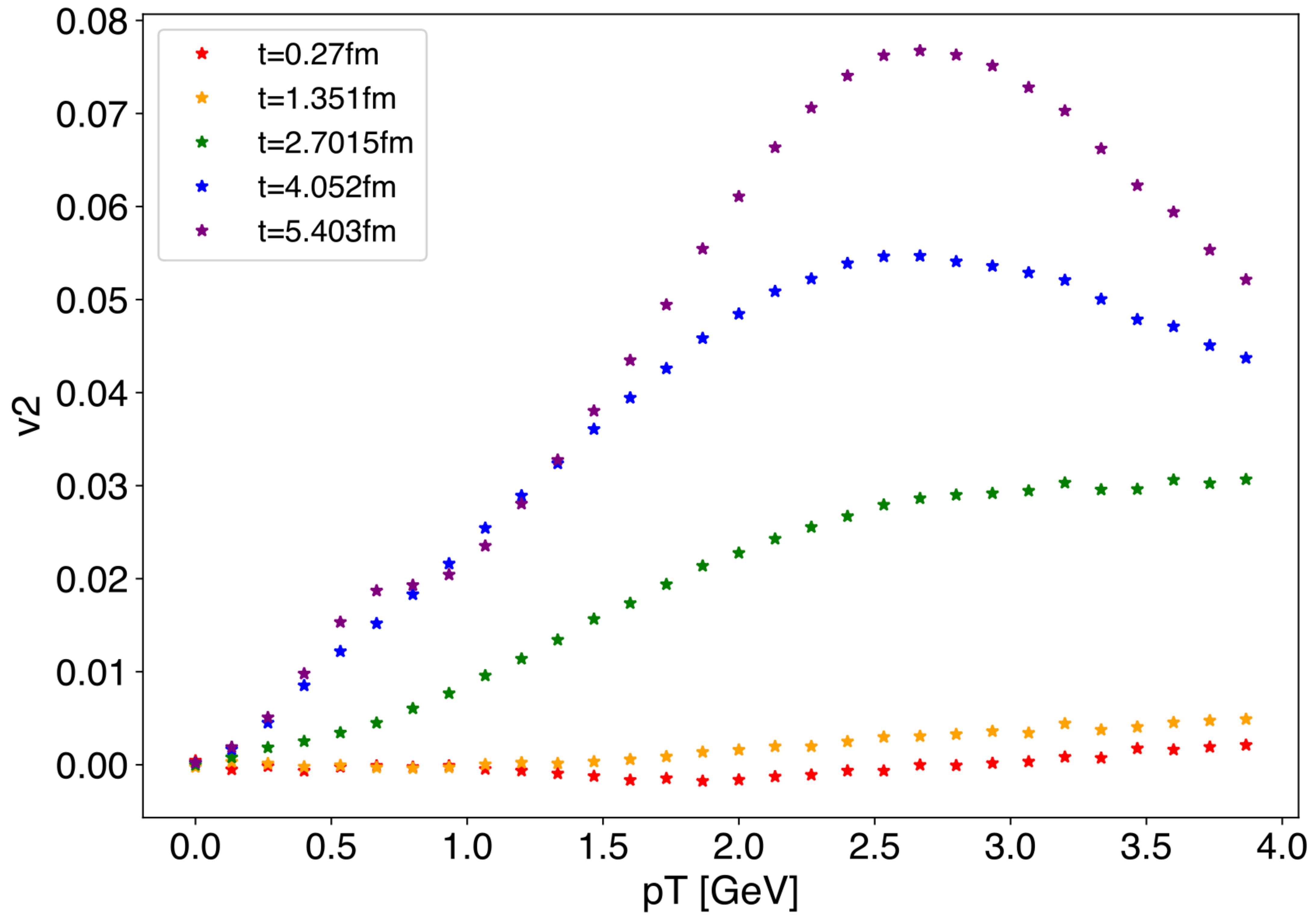

➡ Heavy quarks interact strongly with the medium

Charmonium Elliptic Flow v_2

Au+Au @ 200 GeV

Preliminary results of v_2 at $\sqrt{s_{NN}} = 200$ GeV, 20-40% centrality

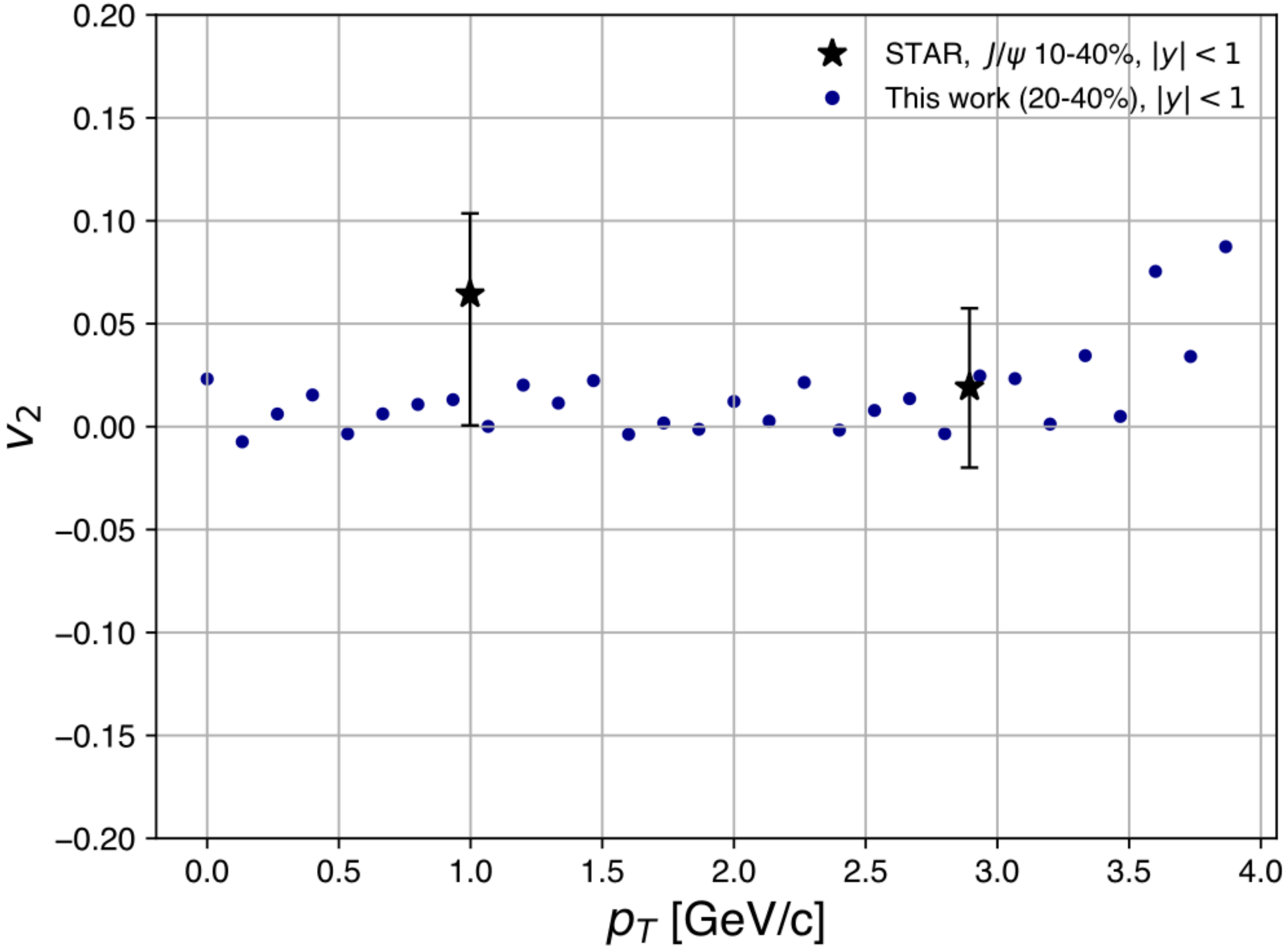

- STAR data: $v_2^{J/\psi}$ consistent with zero within uncertainties
- At RHIC: regeneration expected subdominant
- primordial J/ψ: weakly coupled to medium $\rightarrow$ $v_2^{J/\psi} \approx 0$
- This work: regeneration only

➡indication of a weak, but non-zero v_2

STAR Collaboration. Measurement of J/Psi Azimuthal Anisotropy in Au+Au Collisions at $\sqrt{s_{NN}}$ = 200 GeV. PRL 111, 052301 (2013)

➡Upper-limit estimate for regeneration-driven $v_2^{J/\psi}$ at RHIC

Charmonium Elliptic Flow v_2

Pb+Pb @ 2.76 TeV

Preliminary results of v_2 at $\sqrt{s_{NN}} = 2.76$ TeV , 20-40% centrality

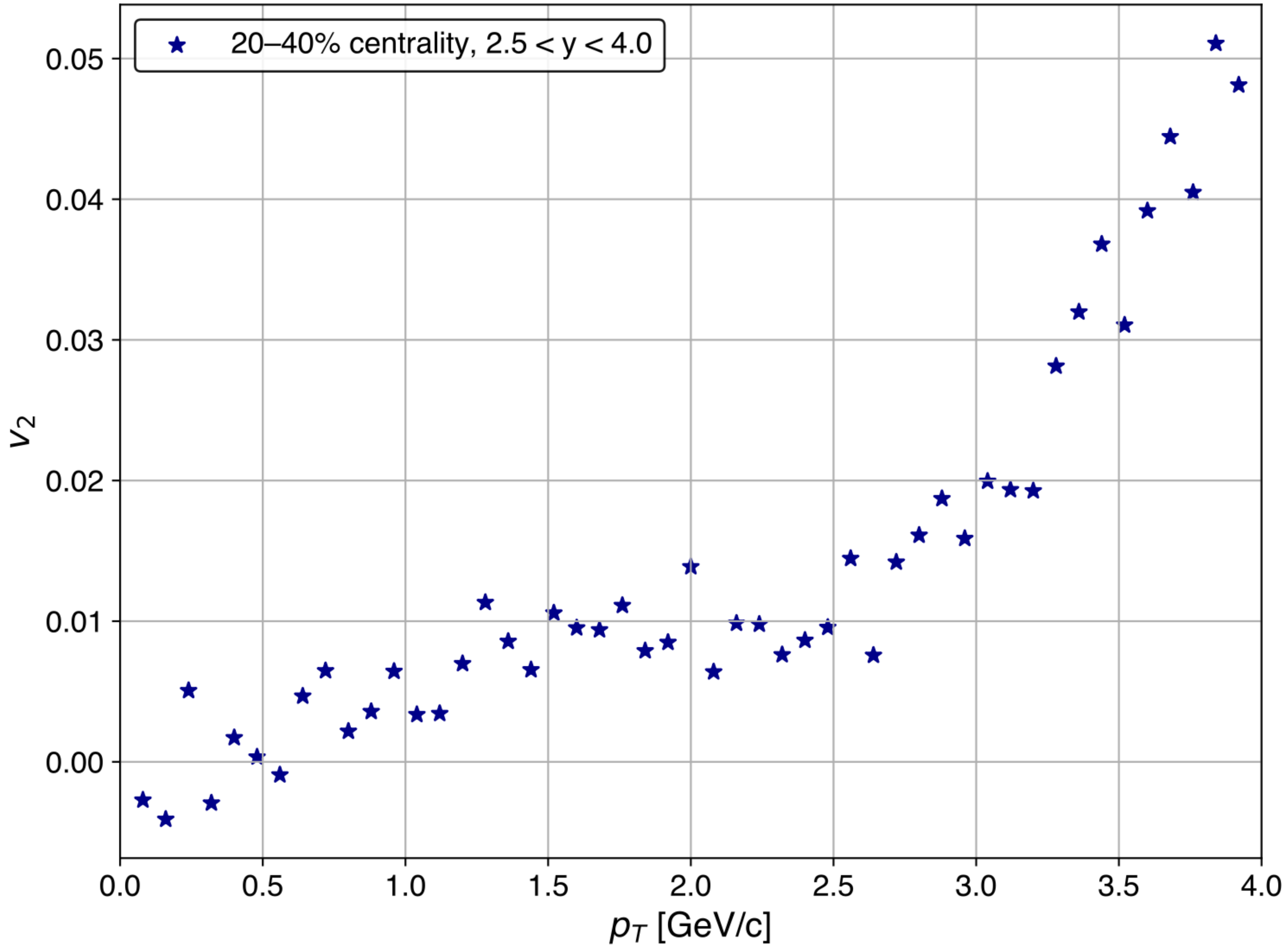

- LHC energy: regeneration dominant → $v_2^{J/\psi} > 0$ expected
- Regenerated J/ψ inherit flow from c and $\bar{c}$
- Our simulation: positive v_2 with increasing p_T
- Detailed p_T-shape not yet reproduced

➡ Expected: follows trend of charm-quark v_2

Charmonium Elliptic Flow v_2

Pb+Pb @ 2.76 TeV

Preliminary results of v_2 at $\sqrt{s_{NN}} = 2.76$ TeV , 20-40% centrality

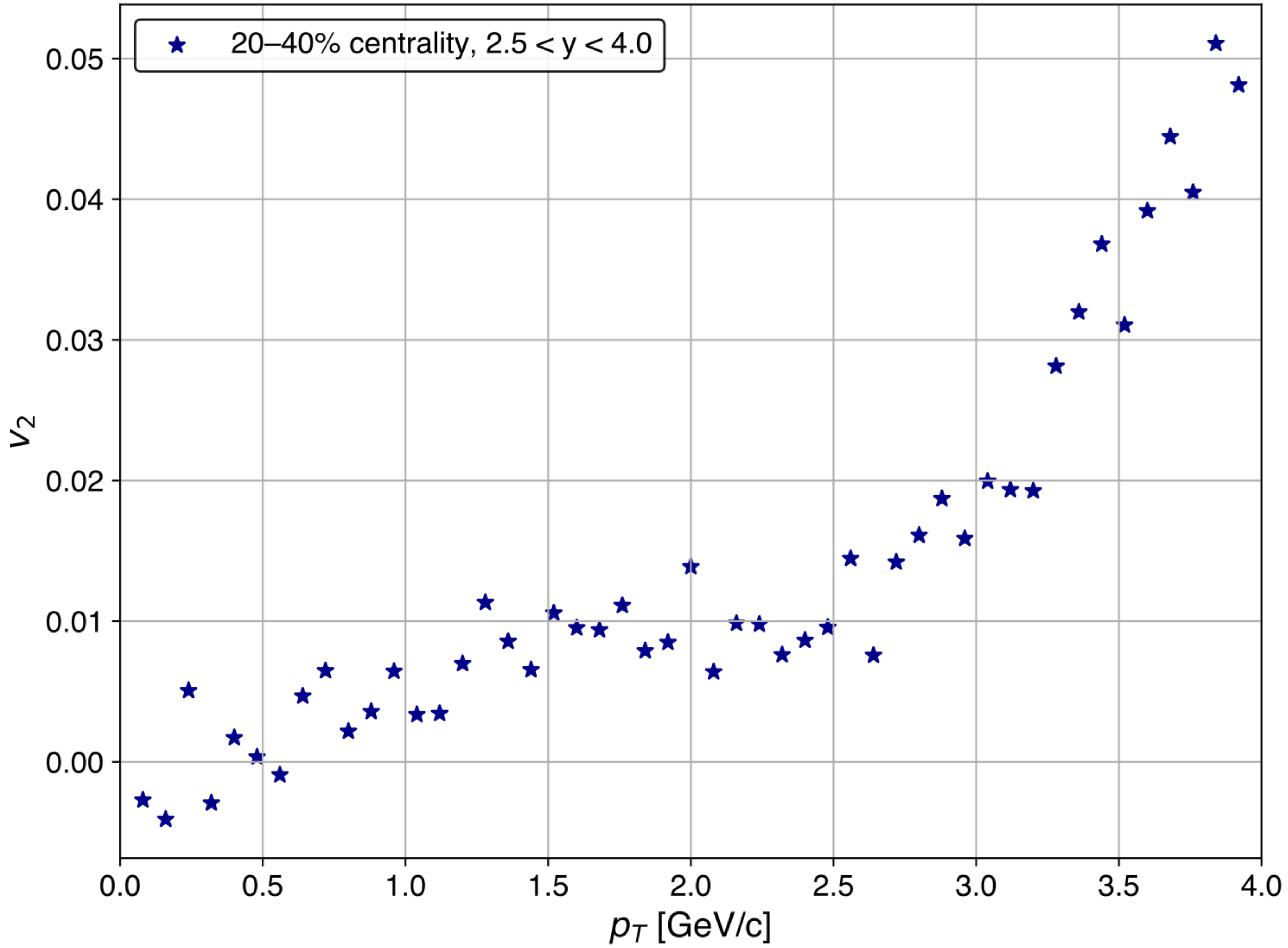

- LHC energy: regeneration dominant → $v_2^{J/\psi} > 0$ expected
- Regenerated J/ψ inherit flow from c and $\bar{c}$
- Our simulation: positive v_2 with increasing p_T
- Detailed p_T-shape not yet reproduced

➡ Expected: follows trend of charm-quark v_2

➡ RHIC: primordial regime → $v_2^{c\bar{c}} \simeq 0$

➡ LHC: regeneration regime → $v_2^{c\bar{c}} > 0$

Conclusions & Outlook

Summary:

- Classical, microscopic model based on Langevin equation to describe charm quarks and charmonium
- Box simulations $\rightarrow$ correct equilibrium limit
- Bound-state formation, dissociation and regeneration occur in the expected manner
- Implementation of fireball model to describe dynamical expansion
  - ➡ J/ψ yield
  - ➡ v_2 of charm and charmonium

Future extensions:

- R_{AA} and statistically robust results for charmonium- v_2
- Include primordial charmonium
- Parametrize fireball to $\sqrt{s_{NN}} = 5.02$ TeV $\rightarrow$ comparison to experimental data
- Hadronization

Backup

Charmonium Yields

Comparison to Statistical Hadronization Model

- Charmonium yield based on the charm quark number N_c in Grand-Canonical Ensemble:

$$N_{c\bar{c}} = \sum_{\alpha} \frac{N_c^2}{V} \frac{g_\alpha}{g_{c^2}} \left(\frac{2\pi}{T}\right)^{3/2} \frac{M_\alpha^{3/2}}{M_c^3} e^{\frac{2M_c - M_\alpha}{T}}$$

with $\alpha = \{\eta_c, J/\psi, \psi', \chi_c\}$, $\lambda_\alpha = \lambda_c^2$

➡ Charmonium yield scales with N_c^2

➡ Deviations at small N_c due to canonical enhancement effects (?)

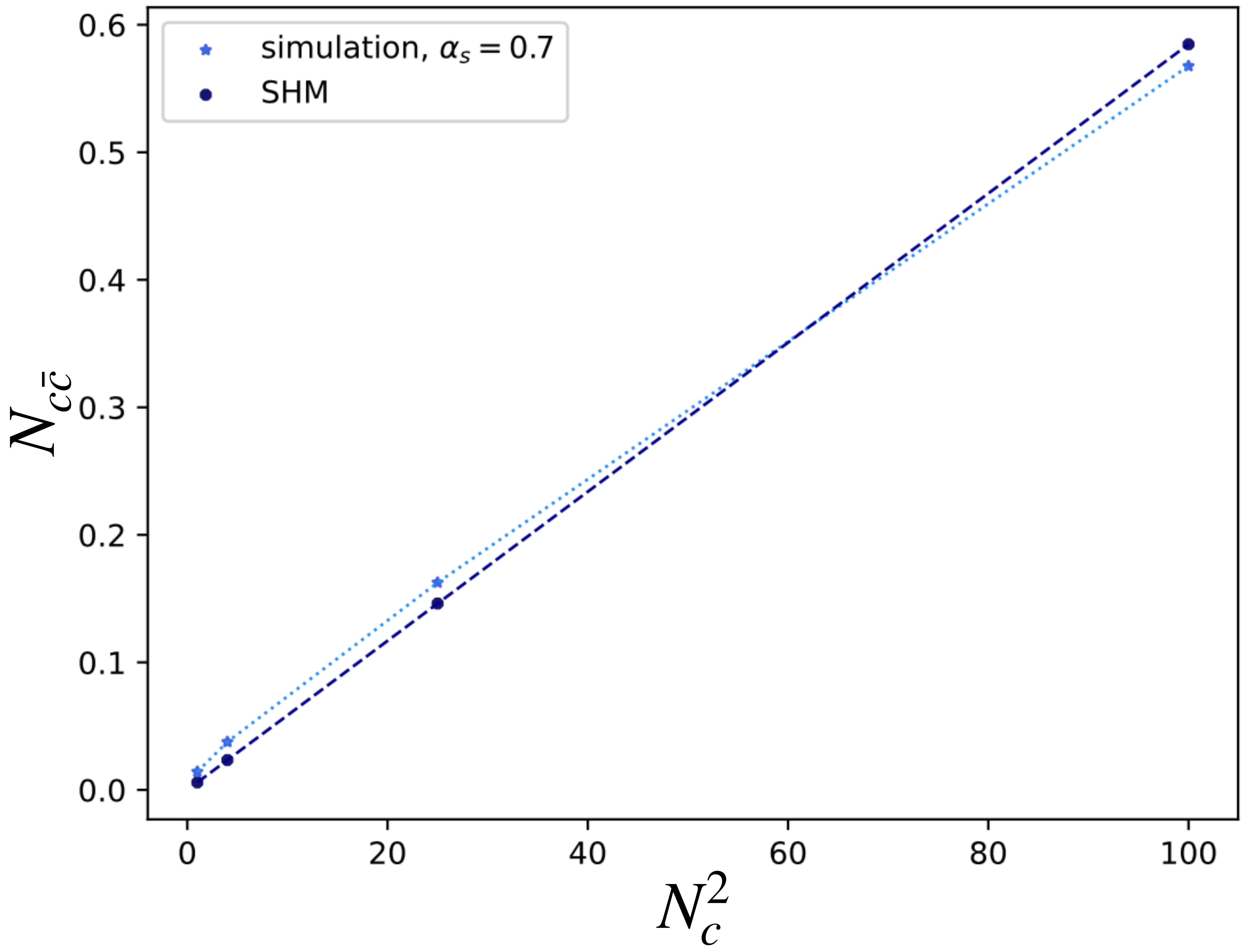

Complex Potential

Concept: finite-temperature field theory

- in-medium propagator of a heavy quark pair → potential acquires imaginary part

$$\mathcal{V}(r) = -\frac{g^2}{4\pi}m_D - \frac{g^2}{4\pi}\frac{\exp(-m_D r)}{r} - i\frac{g^2 T}{4\pi}\phi(m_D r) \rightarrow \phi(x) = 2\int_0^\infty dz \frac{z}{(z^2+1)^2}\left[1 - \frac{\sin(zx)}{zx}\right]$$

- ϕ: arises when computing Landau damping contributions to the potential in finite-temperature QCD
- encodes how dissociation width depends on distance:
- Short distances ($x = m_D \ll 1$):

➡ $\phi(x) \sim x$, small imaginary part → little dissociation → bound state tightly localised, less exposed to the medium

➡ $\phi(x) \rightarrow const.$, imaginary part saturates → pair is far apart → strong decoherence → more likely to dissolve

Strong Coupling of Potential

Influence on Number of Bound States

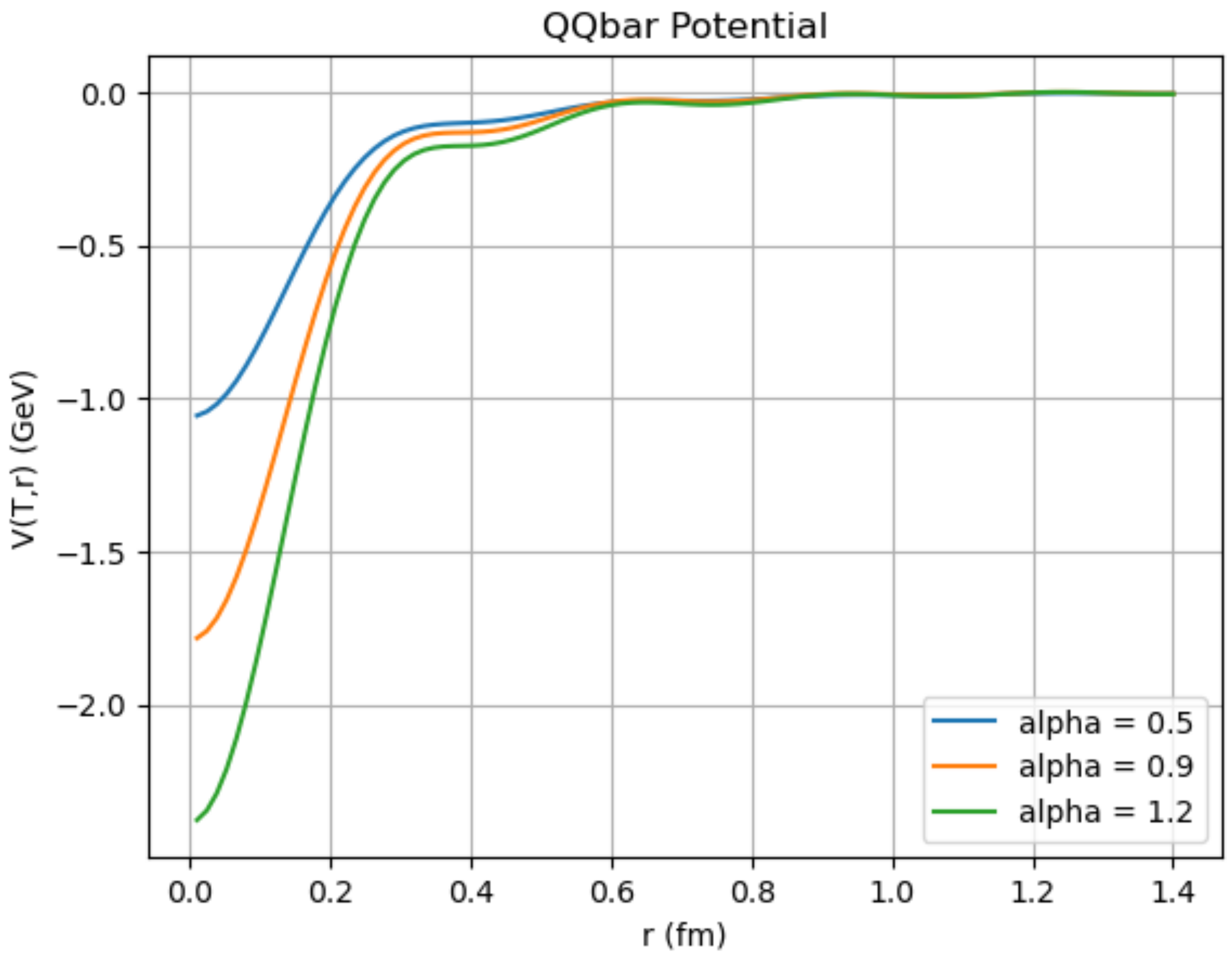

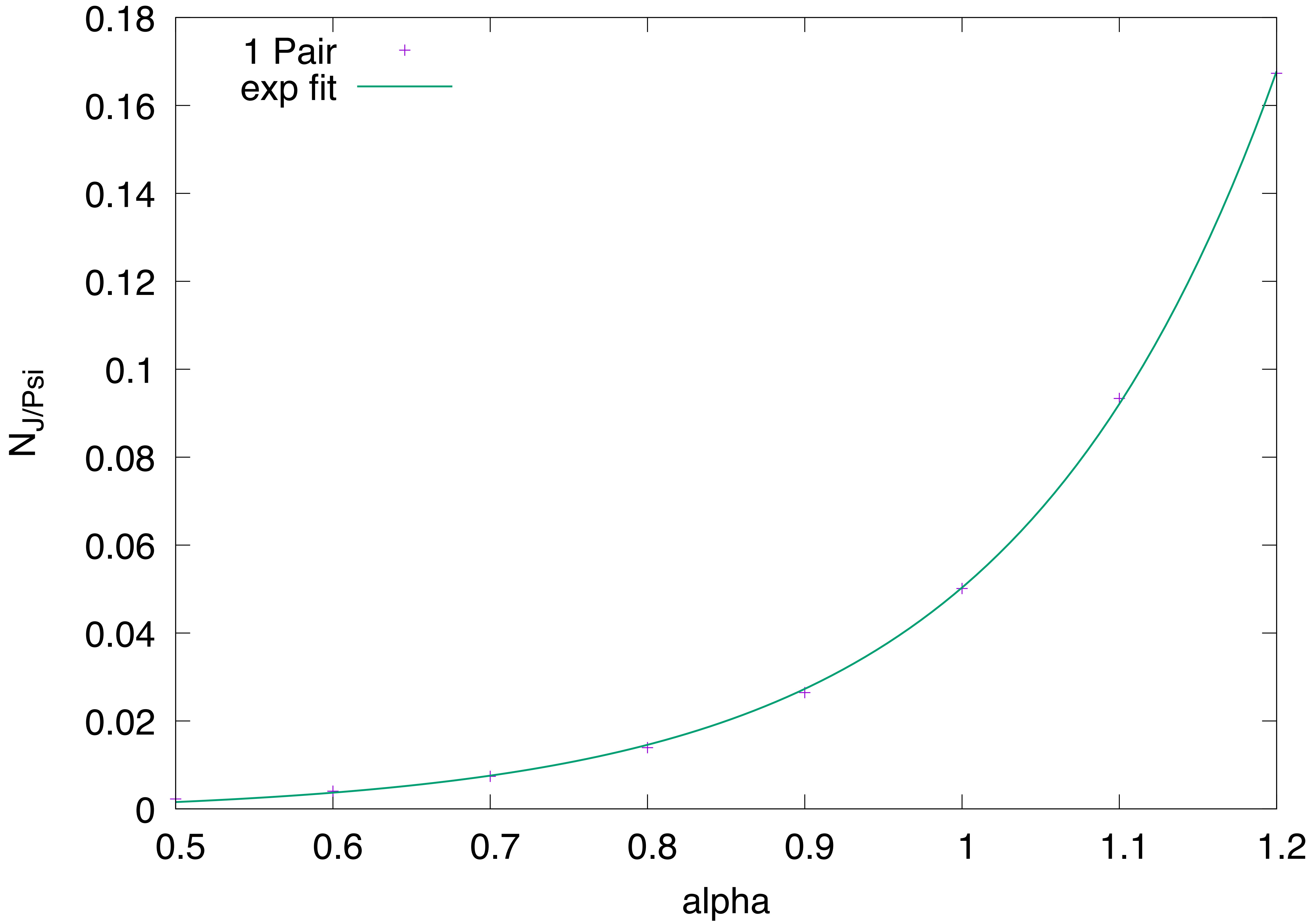

Parametrization of the Fireball

RHIC (20-40%), v_2

- Choice of parameters in fireball model by fitting results to experimental data
- Elliptic flow v_2 of K_S and ϕ from STAR

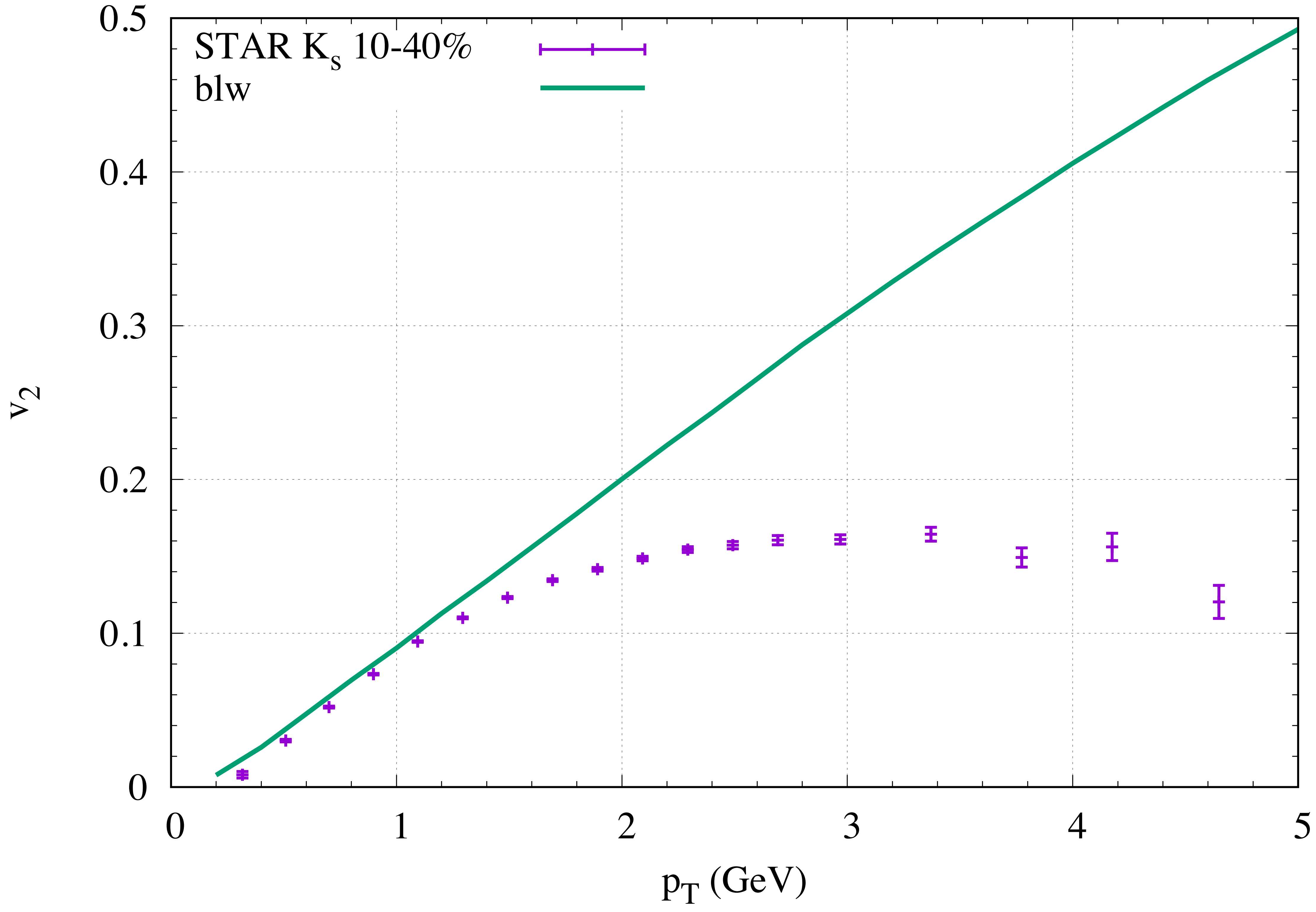

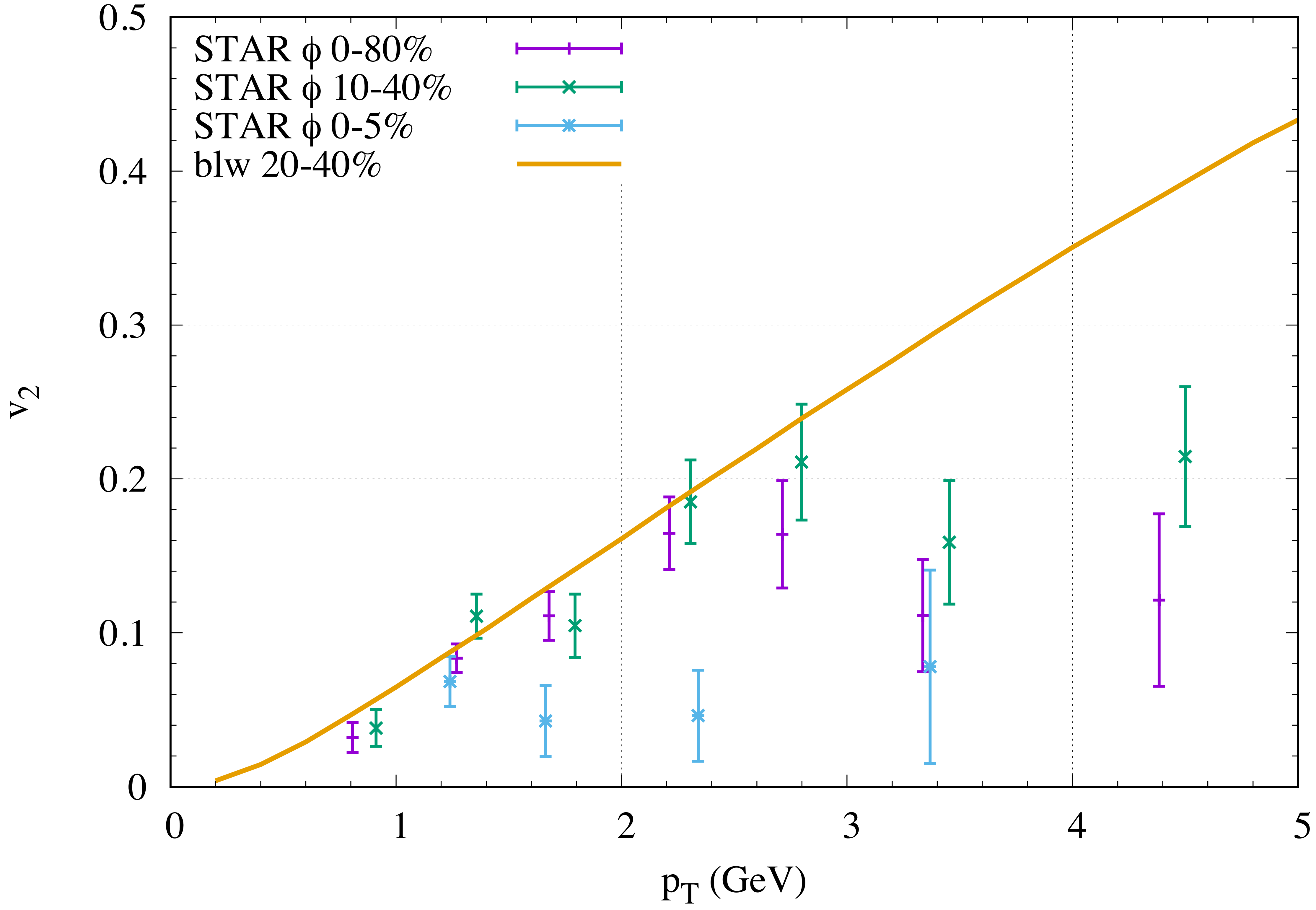

Parametrization of the Fireball

RHIC (20-40%), p_T

p_T-spectra of p and ϕ from STAR